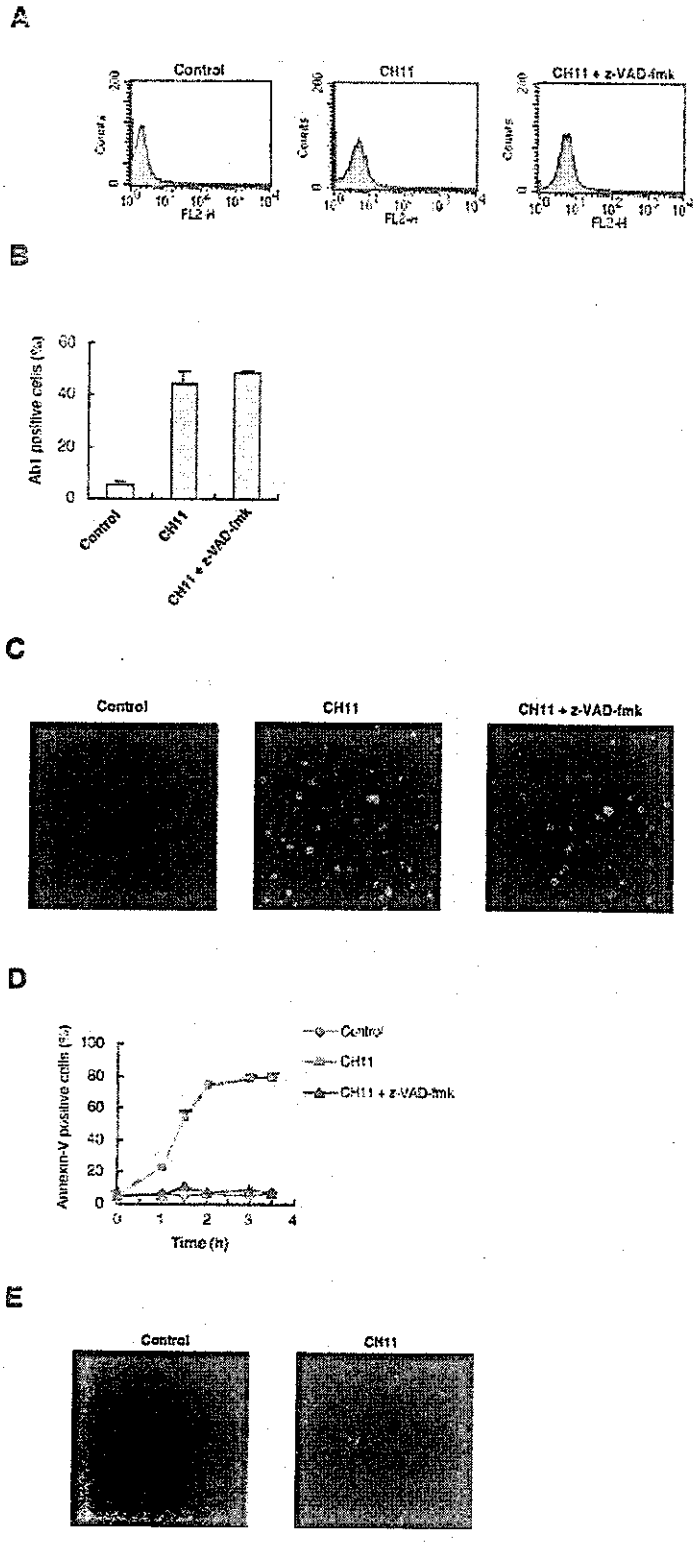

FIG. 2. **Exposure of the N terminus of Bak in Jurkat cells treated with CH11 in the presence of z-VAD-fmk.** *A–C*, Jurkat cells were treated without or with CH11 (0.5 μg/ml) for 30 min in the presence or absence of z-VAD-fmk (100 μM). Then immunostaining was performed with anti-Bak Ab1 antibody, followed by FACS analysis (*A* and *B*) or confocal microscopy examination (*C*). In *B*, Ab1-positive cells were counted by FACS analysis. Data are shown as the mean ± S.E. (n = 3). *D*, inhibition of CH11-induced apoptosis by z-VAD-fmk (100 μM). *E*, JB6 cells were treated without or with CH11 (0.5 μg/ml) for 1 h, and then immunostaining was performed with anti-Bak Ab1 antibody followed by confocal microscopy examination.

in other cell lines. As was the case for HeLa cells exposed to CH11, CH11-stimulated Jurkat cells displayed an increase of immunoreactivity to Ab1 antibody, which was not affected by z-VAD-fmk as assessed by FACS and confocal microscopy (Fig. 2, *A–C*). The dose of z-VAD-fmk used (100 μM) completely inhibited the activation of caspases, cleavage of Bid, and cell death (Fig. 2*D* and data not shown). Furthermore, we also found that exposure of the N terminus of Bak occurred in Fas-stimulated JB6 cells, a caspase-8-deficient subline of Jurkat cells (Fig. 2*E*). These results suggest that Fas stimulation could activate a caspase-8-independent signaling pathway and induce exposure of the N terminus of Bak, but this change of

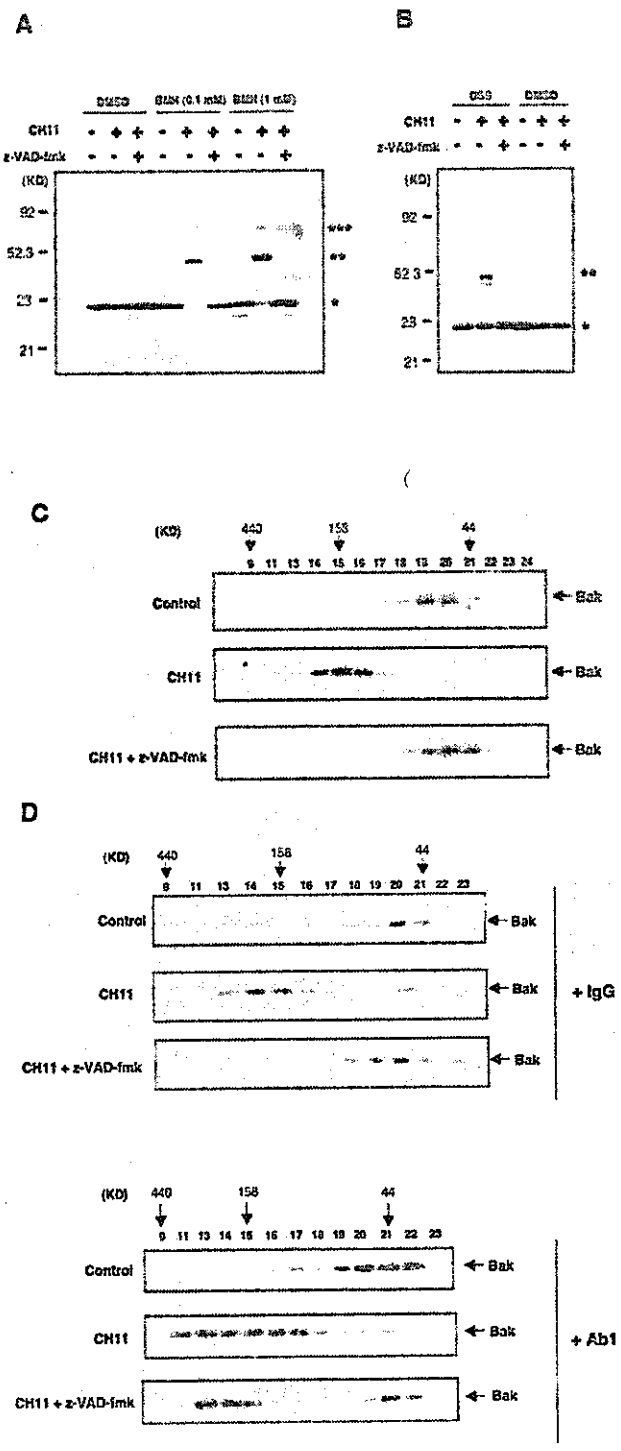

FIG. 3. **Oligomerization of Bak in Fas-stimulated Jurkat cells, and its inhibition by z-VAD-fmk.** *A*, Jurkat cells were treated without or with CH11 (0.5 μg/ml) in the presence or absence of z-VAD-fmk (100 μM) for 2 h, harvested, and incubated with a cross-linker, BMH (uncleavable), or Me_2SO (the solvent) for 30 min at room temperature. Oligomerization of Bak was detected by Western blotting. The *asterisks* denote monomeric, dimeric, trimeric Bak, respectively. *B*, Jurkat cells were treated with CH11 (0.5 μg/ml) in the presence or absence of z-VAD-fmk (100 μM) for 2 h, followed by lysis and incubation with 1 mM DSS or Me_2SO for 30 min at room temperature. Oligomerization of Bak was assayed by Western blotting. *C* and *D*, Jurkat cells were treated with CH11 (0.5 μg/ml) for 1 h in the presence or absence of z-VAD-fmk (100 μM). The lysates were incubated without (*C*) or with (*D*) anti-Bak Ab1 antibody or normal mouse IgG for 3 h and then analyzed by gel filtration column chromatography. The distribution of Bak was analyzed by Western blotting.

Bak was not sufficient for full activation.

Fas-induced Caspase-independent Exposure of the N Terminus of Bak Is Separable from Oligomerization—Previous studies indicated that Bak undergoes homo-oligomerization in apoptotic cells (11, 18, 28). Because its oligomerization is correlated with the release of cytochrome *c* from the mitochondria (11), it is thought to represent activation. Oligomerization of Bak can be detected either by using a protein cross-linker or by gel filtration column chromatography (11, 15). With these procedures, we showed that Bak was oligomerized in CH11-treated cells and this change was inhibited by z-VAD-fmk (Fig. 3, *A–C*), indicating that its oligomerization was dependent on the activation of caspases. These results suggested that caspase-independent exposure of the N terminus of Bak was separable from its oligomerization.

We further confirmed caspase-8-independent exposure of the N terminus of Bak by gel filtration. Lysates of Jurkat cells treated with or without CH11 in the presence or absence of z-VAD-fmk were incubated with Ab1 antibody or normal mouse IgG before being subjected to gel filtration column chromatography. If Bak binds to Ab1 antibody, it would be eluted in the fractions that correspond to the larger molecular size proteins. As shown in Fig. 3*D*, when the sample from untreated cells was incubated with Ab1 antibody and then applied to the column, Bak was detected in the fractions corresponding to low molecular weight proteins, as was the case without incubation with Ab1 antibody (Fig. 3*C*) or after incubation with control normal mouse IgG (Fig. 3*D*, *upper panel*), indicating no exposure of the N terminus of Bak. When the sample from CH11-treated cells was incubated with Ab1 antibody, Bak shifted to the larger molecular weight fractions, which were larger than that when the sample was incubated with normal mouse IgG or without Ab1 antibody (Fig. 3, *C* and *D*), suggesting that the N terminus was exposed in apoptotic cell lysates. When lysates from cells treated with CH11 in the presence of z-VAD-fmk were incubated with Ab1 antibody, the Bak peak was found in fractions that corresponded to both high and low molecular weight proteins (Fig. 3*D*, *lower panel*), indicating that Bak was recognized by Ab1 antibody in cells treated with CH11 in the presence of z-VAD-fmk. This result is consistent with our immunostaining data. Taken together, these observations suggest that Fas stimulation induces exposure of the N terminus of Bak in a caspase-8-independent manner and that N-terminal exposure is separable from the oligomerization of Bak.

Exposure of the N Terminus of Bak Makes Cells More Sensitive to Apoptotic Stimuli—The results described above showed that Fas-dependent/caspase-independent exposure of the N terminus of Bak did not lead to its full activation. Did such exposure of N terminus have any biological significance? We hypothesized that full activation of Bak requires at least two steps, *i.e.* exposure of the N terminus, followed by oligomerization, and that Bak with N-terminal exposure might be in a "primed state." It should be noted that exposure of the N terminus can be mediated by both caspase-8-dependent and independent mechanisms. If this hypothesis is correct, cells in which the N terminus of Bak is exposed may be more sensitive to subsequent death stimuli. To test this possibility, Jurkat cells were pretreated with CH11 in the presence of z-VAD-fmk for 2 h to "prime" Bak, and then were exposed to 10 μM VP-16 (etoposide) in the presence of z-VAD-fmk. z-VAD-fmk did not inhibit transmission of VP-16-induced death signals to the mitochondria or release of cytochrome *c* from the mitochondria

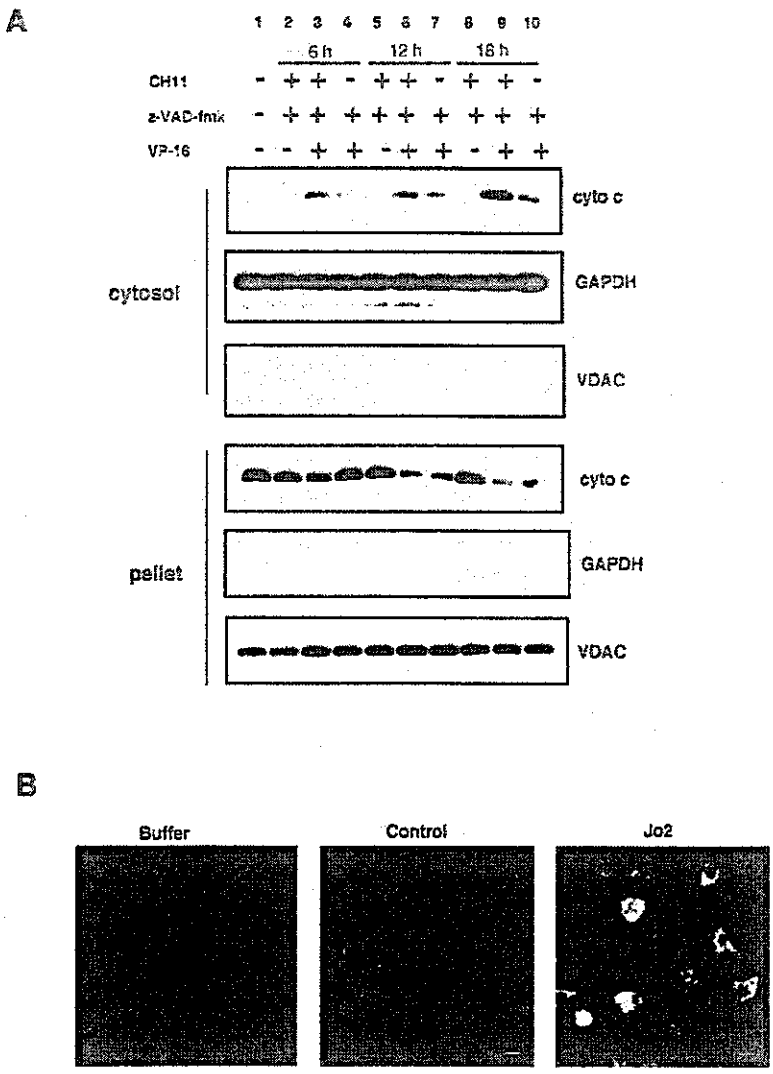

FIG. 4. **Increased susceptibility to VP-16-induced apoptosis of cells possessing Bak with N-terminal exposure.** *A*, Jurkat cells were treated with or without CH11 (0.5 μg/ml) in the presence of z-VAD-fmk (100 μM) for 2 h, followed by incubation with VP-16 (10 μM) in the presence of z-VAD-fmk for the indicated times. The cells were fractionated into cytosolic (cytosol) and organellar (pellet) fractions, and then analyzed by Western blotting with anti-cytochrome *c* antibody. Glyceraldehyde-3-phosphate dehydrogenase (*GAPDH*) and voltage-dependent anion channel protein (*VDAC*) were monitored to verify successful fractionation and as loading controls. *B*, cytosol was prepared from caspase-$8^{-/-}$ MEFs treated without (*control*) or with Jo2 (0.5 μg/ml) for 16 h and was added to HeLa cells that had been permeabilized by incubation with digitonin (20 μg/ml) for 3 min at room temperature. After incubation for 10 min at 37 °C, immunostaining was done with anti-Bak Ab1 antibody. As a negative control, isotonic buffer was added instead of cytosol. *Scale bar* = 10 μm. *C*, caspase-$8^{-/-}$ MEFs were treated with Jo2 (0.5 μg/ml) or TNFα (10 ng/ml) for 16 h, followed by incubation with 10 μM VP-16 for the indicated times. Apoptotic cells were detected by Annexin-V staining. Data are shown as the mean ± S.E. (n = 3). *D*, caspase-$8^{-/-}$ MEFs were pretreated as described in *C*, followed by incubation with 10 μM VP-16 for 24 h, and then stained with Hoechst 33342. *Scale bar* = 10 μm. *E*, caspase-$8^{-/-}$ MEFs were treated with Jo2 (0.5 μg/ml) or TNFα (10 ng/ml) for 16 h, followed by incubation with 10 μM VP-16 for 18 h. The cells were fractionated into cytosolic (cytosol) and organellar (pellet) fractions, and then extracts were subjected to Western blotting with anti-cytochrome *c* antibody. *F*, caspase-$8^{-/-}$ MEFs were treated with Jo2 (0.5 μg/ml) or TNFα (10 ng/ml) for 16 h, followed by incubation with 10 μM VP-16 for 18 h. After lysis, the activation of caspase-3 was assayed by Western blotting.

(data not shown). VP-16 induced the release of only a small amount of cytochrome *c* from the mitochondria in the cells without CH11 pretreatment (Fig. 4*A*, *lanes 4*, *7*, and *10*). In contrast, a large amount of cytochrome *c* was released after cells were pretreated with CH11/z-VAD-fmk and then exposed to VP-16 (Fig. 4*A*, *lanes 3*, *6*, and *9*). This result indicates that, although CH11 alone could not induce cytochrome *c* release in the presence of z-VAD-fmk (Fig. 4*A*, *lanes 2*, *5*, and *8*), it sensitized cells to subsequent treatment with VP-16, suggesting that Bak with N-terminal exposure might represent "primed Bak."

We also examined whether Fas-induced caspase-independent exposure of the N terminus of Bak could sensitize cells to apoptotic death. Because z-VAD-fmk inhibits apoptosis, we could not use it in experiments that assayed cell death. Therefore, we employed caspase-8-deficient murine embryonic fibroblasts (MEFs), which are completely resistant to death receptor-mediated apoptosis (29). First, we investigated whether stimulation of Fas with agonistic anti-mouse Fas antibody Jo2 induced exposure of the N terminus of Bak in caspase-8-deficient MEFs. Because no antibody was available to recognize a conformational change of mouse Bak, we employed an *in vitro* assay system using HeLa cells permeabilized by digitonin. Lysates derived from caspase-$8^{-/-}$ MEFs treated with or without Jo2 were added to digitonin-permeabilized HeLa cells, and then immunostaining was performed with Ab1 antibody. As shown in Fig. 4*B*, lysate from Jo2-treated caspase-$8^{-/-}$ MEFs, but not lysate from untreated cells, caused an increase of Ab1 immunoreactivity. This indicated that, as in Jurkat and HeLa cells, one or more factors that induced exposure of the N terminus of Bak existed in the lysates of Jo2-treated caspase-$8^{-/-}$ MEFs and, although not proved, suggested that Bak entered a primed state in caspase-$8^{-/-}$ MEFs after Jo2 treatment.

To examine whether Jo2-treated caspase-$8^{-/-}$ MEFs, in which Bak was considered to exist in a primed state, were more sensitive to death stimuli, we pretreated caspase-$8^{-/-}$ MEFs with Jo2 alone for 16 h, followed by exposure to 10 μM VP-16. Note that cycloheximide was not added here, because cycloheximide inhibited VP-16-induced apoptosis in MEFs (data not shown). As shown in Fig. 4 (*C* and *D*), pretreatment with Jo2 enhanced VP-16-induced apoptosis. The same result was also obtained with TNFα instead of Jo2 (Fig. 4, *C* and *D*). After 18 h of exposure to VP-16, Jo2- or TNFα-treated cells exhibited release of cytochrome *c* into the cytosol and activation of caspase-3, whereas untreated cells did not show any release of cytochrome *c* or caspase-3 activation at this time (Fig. 4, *E* and *F*). Consistent with a previous report (29), Jo2 or TNFα alone did not induce cytochrome *c* release (data not shown) or death of caspase-$8^{-/-}$ MEFs (Fig. 4, *C* and *D*). These results indicate

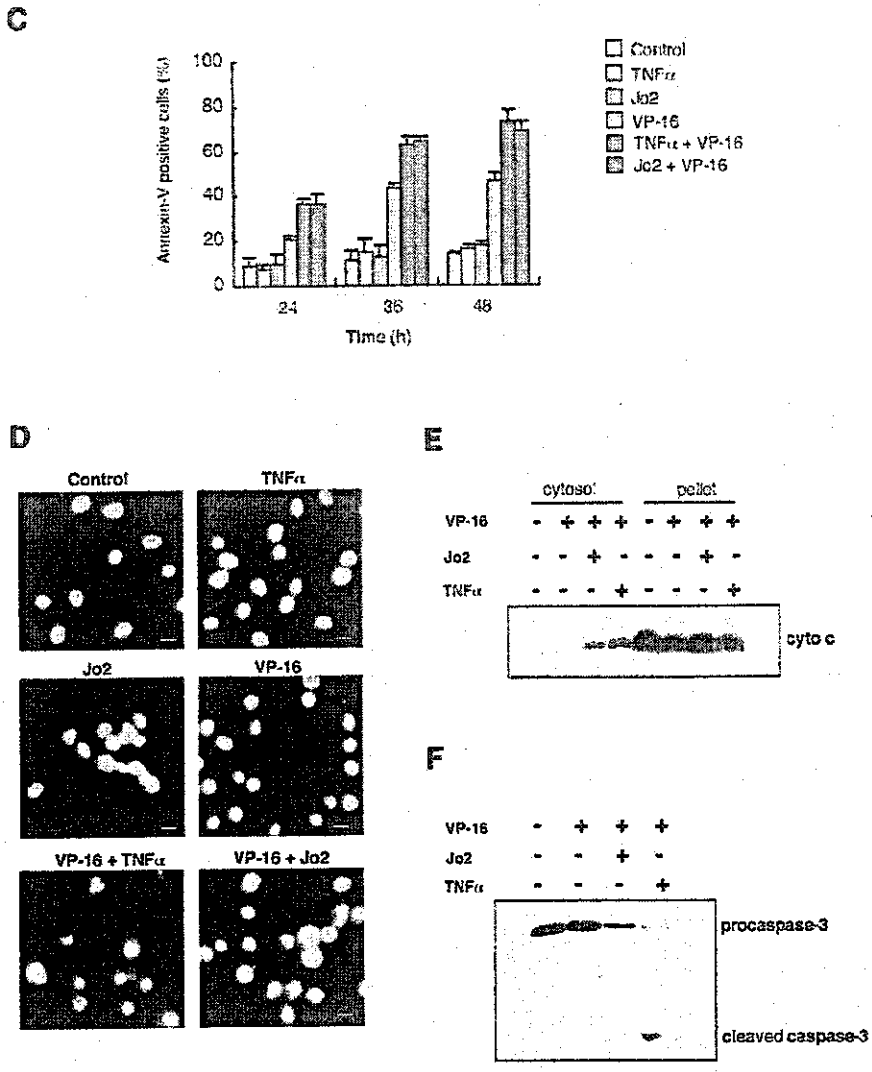

FIG. 4—*continued*

that Fas stimulation without caspase-8 activation could sensitize cells to apoptotic death.

Cytosol from Cells with Primed Bak Enhances Bid-induced Release of Cytochrome c from Isolated Mitochondria—To assess whether Fas stimulation without caspase-8 activation (leading to exposure of the N terminus of Bak) could sensitize the mitochondria to apoptotic signals, we used an *in vitro* system with mitochondria isolated from rat livers. The mitochondria were incubated for 5 min with cytosol derived from caspase-$8^{-/-}$ MEFs with or without Jo2 treatment, followed by incubation with rBid (30 μg/ml) for an additional 20 min. Release of cytochrome *c* was detected by Western blotting. As shown in Fig. 5, treatment with rBid induced the release of cytochrome *c* from isolated mitochondria, and preincubation with cytosol obtained from untreated cells only slightly promoted the release of cytochrome *c*, whereas preincubation with cytosol from treated cells markedly promoted its release. The incubation of isolated mitochondria with cytosol alone only induced slight release of cytochrome *c* (Fig. 5). These results indicate that Fas stimulation without caspase-8 activation induces a signal that could sensitize the mitochondria to apoptotic stimuli.

Bak Has an Essential Role in the Increased Susceptibility to VP-16 of Cells Possessing Bak with Caspase-8-independent N-terminal Exposure—To investigate whether the increased susceptibility to VP-16 of Jo2- or TNFα-pretreated caspase-$8^{-/-}$ MEFs was due to primed Bak, we used RNA interference to silence the expression of Bak in caspase-$8^{-/-}$ MEFs. Cells were transfected with Bak siRNA, or GFP siRNA (as a negative control), and then the expression of Bak was examined by Western blotting. As shown in Fig. 6*A*, Bak expression decreased to a nearly undetectable level after treatment with siRNA for Bak, and the silencing effect lasted for more than 72 h, whereas the Bax level remained unchanged. As observed above, Jo2- or TNFα-pretreated caspase-$8^{-/-}$ MEFs displayed an increase of susceptibility to VP-16-induced apoptosis when transfected with control GFP siRNA, whereas Jo2 or TNFα could not sensitize these cells to VP-16 after Bak was eliminated by siRNA treatment (Fig. 6*B*). It should be noted that silencing of Bak did not affect VP-16-induced apoptosis (Fig. 6*B*), which was probably mediated by Bax. In contrast, when Bax was eliminated by using Bax siRNA (Fig. 6*C*), the susceptibility of Jo2- or TNFα-pretreated caspase-$8^{-/-}$ MEFs to VP-16 was unchanged (Fig. 6*D*). Taken together, these data indicate that Bak plays an important role in the increased susceptibility to VP-16 of Jo2- or TNFα-treated cells.

A Staurosporine-sensitive Signal Elicited by Fas Ligation Is Responsible for Caspase-independent Exposure of the N Terminus of Bak—In addition to the well characterized caspase-8-de-

pendent apoptotic pathway, Fas stimulation has also been shown to activate other signaling pathways that lead to the activation of extracellular signal-regulated kinase (ERK) (30–32), c-Jun N-terminal kinase (JNK) (33), and tyrosine kinases (34). To obtain some insights into the signaling pathways involved in exposure of the N terminus of Bak in a caspase-8-independent fashion after Fas stimulation, we employed several kinase inhibitors to examine whether N-terminal exposure induced by CH11 in the presence of z-VAD-fmk could be blocked in HeLa cells. Among the inhibitors tested, PD98059 (ERK), SP600125 (JNK), and genistein (tyrosine kinases) did not affect Fas-induced caspase-8-independent exposure of the N terminus of Bak (data not shown). However, the pan kinase inhibitor staurosporine (STS) (10 nM) impaired the increase of anti-Bak Ab1 immunoreactivity induced by CH11 in the presence of z-VAD-fmk (Fig. 7*A*), although STS did not inhibit the increase of anti-Bak Ab1 immunoreactivity induced by CH11 alone (Fig. 7*A*). This indicates that at least two independent pathways are involved in exposure of the N terminus of Bak after Fas stimulation, one that is caspase-8/Bid-independent and involves an STS-sensitive kinase and another that is the well characterized caspase-8/Bid pathway. The inhibitory effect of STS was also confirmed by our *in vitro* permeabilized cell system. As shown in Fig. 7*B*, consistent with the *in vivo* results, cytosol derived from cells treated with CH11 in the presence of z-VAD-fmk together with STS could not induce exposure of the N terminus of Bak, whereas cytosol from cells treated with CH11 in the presence of z-VAD-fmk and rBid induced exposure of the N terminus. Furthermore, cytosol from cells treated with CH11/z-VAD-fmk/STS also failed to enhance rBid-induced cytochrome *c* release from isolated mitochondria (Fig. 7*C*). These results indicate that an STS-sensitive kinase plays a role in caspase-independent exposure of the N terminus of Bak after Fas stimulation.

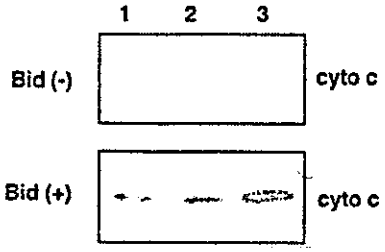

FIG. 5. **Enhancement of Bid-induced release of cytochrome *c* from isolated mitochondria by cytosol from cells with prior exposure of the N terminus of Bak.** Cytosol derived from untreated caspase-$8^{-/-}$ MEFs (*lane 2*) and caspase-$8^{-/-}$ MEFs treated with 0.5 μg/ml Jo2 for 16 h (*lane 3*) were incubated with mitochondria isolated from rat livers for 5 min, followed by incubation with (*lower panel*) or without (*upper panel*) rBid (30 μg) for a further 20 min. As a negative control, isotonic buffer was added instead of cytosol (*lane 1*). Release of cytochrome c was determined by Western blotting.

DISCUSSION

In response to various apoptotic stimuli, Bax and Bak undergo conformational changes such as exposure of their N terminus and homo-oligomerization: the homo-oligomers are considered to be active forms that induce permeabilization of the outer mitochondrial membrane, a process that is central to apoptotic death (3, 4). During death receptor-mediated apoptosis (type II cells), formation of the active forms of Bax and Bak depends on activation of caspase-8 and subsequent cleavage of Bid, because both caspase-8 and Bid are essential for these modes of apoptosis (11, 29, 35). In the present study, however, we showed that, in the absence of caspase-8 activa-

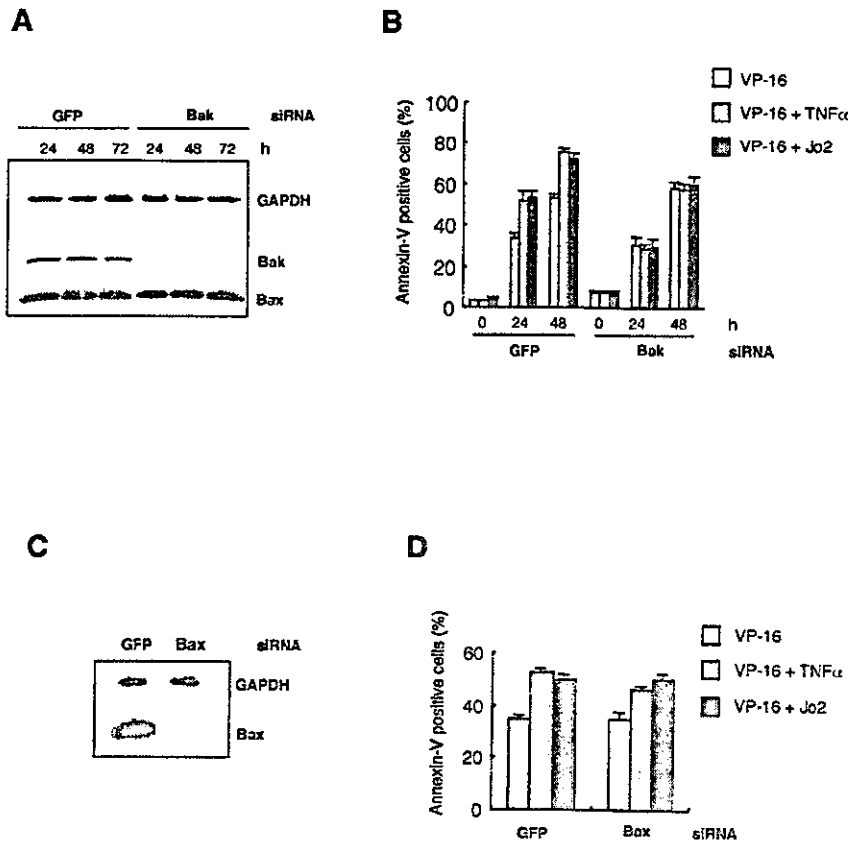

FIG. 6. **Requirement of Bak for the Jo2-induced increased susceptibility to VP-16 of caspase-$8^{-/-}$ MEFs.** *A*, caspase-$8^{-/-}$ MEFs were transfected with Bak siRNA (10 μg) or GFP siRNA (10 μg). Expression of Bak, Bax, and glyceraldehyde-3-phosphate dehydrogenase was detected at the indicated times after the last transfection of siRNA by Western blotting. *B*, siRNA-transfected caspase-$8^{-/-}$ MEFs were treated with Jo2 (0.5 μg/ml) or TNFα (10 ng/ml) for 16 h, followed by incubation with 10 μM VP-16 for the indicated times. Apoptotic cells were detected by Annexin-V staining. Data are shown as the mean ± S.E. (n = 3). *C*, caspase-$8^{-/-}$ MEFs were transfected with Bax siRNA (10 μg) or GFP siRNA (10 μg). Expression of Bax and glyceraldehyde-3-phosphate dehydrogenase was detected 24 h after the last transfection by Western blotting. *D*, siRNA-transfected caspase-$8^{-/-}$ MEFs were treated with Jo2 (0.5 μg/ml) or TNFα (10 ng/ml) for 16 h, followed by incubation with 10 μM VP-16 for 24 h. Apoptotic cells were detected by Annexin-V staining. Data are shown as the mean ± S.E. (n = 3).

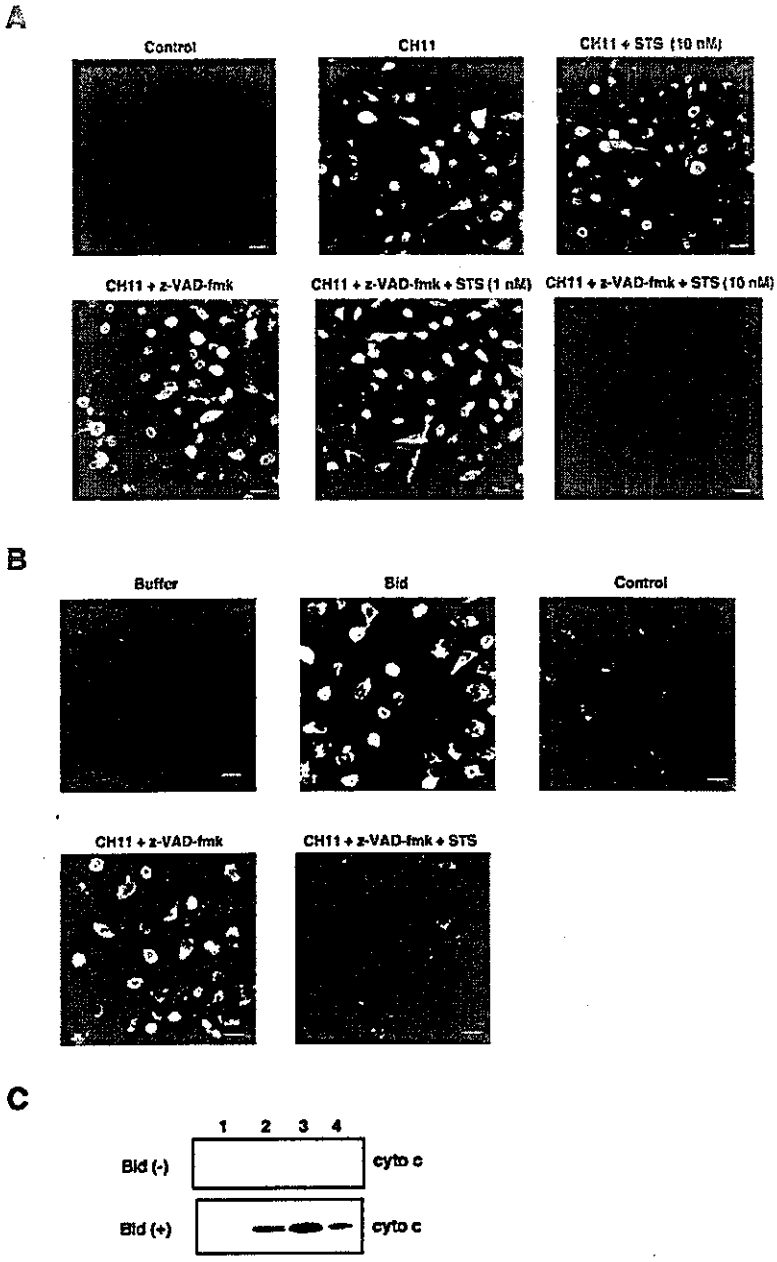

FIG. 7. **Inhibition by STS of caspase-8-independent exposure of the N terminus of Bak induced by Fas.** *A*, HeLa cells were treated as indicated for 2 h, and then were immunostained with anti-Bak Ab1 antibody. *Scale bar* = 20 μm. *B*, digitonin-permeabilized HeLa cells were incubated for 10 min with cytosol derived from HeLa cells with or without CH11/z-VAD-fmk treatment in the presence or absence of STS, followed by immunostaining with monoclonal anti-Bak Ab1 antibody. Isotonic buffer and rBid (0.5 μg) was added instead of cytosol as the negative and positive control, respectively. *Scale bar* = 10 μm. *C*, mitochondria isolated from rat livers were incubated for 5 min with isotonic buffer (*lane 1*), cytosol derived from untreated HeLa cells (*lane 2*), cytosol from HeLa cells treated with CH11 (0.5 μg/ml) and z-VAD-fmk (100 μM) in the absence (*lane 3*) or presence of STS (10 nM) (*lane 4*), followed by incubation with (*lower panel*) or without (*upper panel*) rBid (30 μg) for a further 20 min. Release of cytochrome *c* was detected by Western blotting.

tion, stimulation of Fas and TNF receptor still induced exposure of the N terminus of Bak, suggesting that N-terminal exposure and homo-oligomerization were separable, which is consistent in principle with the previous report that activation of Bak proceeds in multiple steps (19). Similar observations have also been reported for Bax (36, 37). Importantly, we also provided evidence that Bak with N-terminal exposure is in a primed state, because cells possessing Bak with N-terminal exposure were more sensitive to subsequent apoptotic stimulation. This may imply that exposure of the N terminus of Bax/Bak is a prerequisite for homo-oligomerization. Because it is known that exposure of the N terminus of Bax/Bak and oligomerization can be induced by tBid (11, 12), which is generated from Bid by active caspase-8 during death receptor-mediated apoptosis, it needs to be determined whether caspase-dependent exposure of the N terminus of Bak (induced via tBid) and caspase-independent exposure during death receptor-induced apoptosis are identical or not. It is also to be determined how significantly caspase-8-independent exposure of the N terminus of Bak contributes to death receptor-mediated apoptosis. This would be answered once a signaling molecule involved in this process has been identified.

In our present study, we found that Fas stimulation induced exposure of the N terminus of Bak not only in HeLa cells, but also in Jurkat cells. This does not seem consistent with the previous observation of Griffiths *et al.* (13). These authors showed that CH11 (1 ng/ml) could not cause exposure of the N terminus of Bak in Jurkat cells. This discrepancy may be due to a difference in CH11 concentration used. In fact, we found that exposure of the N terminus of Bak did not occur when CH11 concentration was lower than 10 ng/ml (data not shown), suggesting that exposure of the N terminus of Bak requires strong signals from death receptors.

What signals are elicited by stimulation of Fas and TNF

receptor, leading to caspase-8-independent exposure of the N terminus of Bak? Recently, caspase-10 has been identified as an alternative mechanism of death receptor-induced cell death (38). However, it is not likely that caspase-10 induced exposure of the N terminus of Bak, because the caspase inhibitor z-VAD-fmk could not suppress Fas-induced exposure of the N terminus in HeLa and Jurkat cells. Furthermore, the caspase-10 gene has not yet been identified in mice. It has been reported that engagement of Fas activates different signaling pathways, leading to activation of ERK (30–32), JNK (33), tyrosine kinase (34), or phosphatidylcholine-specific phospholipase C (39). It is possible that any of these caspase-independent signaling pathways could transmit a signal to mitochondrial Bak. The present study showed that a nonspecific protein kinase inhibitor, STS, actually inhibited Fas-induced exposure of the N terminus of Bak in the presence of z-VAD-fmk, but not inhibitors of ERK, JNK, or tyrosine kinases. Although further studies are necessary for identification of the kinase(s) responsible for Fas-induced caspase-8-independent exposure of the N terminus of Bak, our results indicate that stimulation of death receptors can elicit two independent signals targeting the mitochondria that regulate Bak activation, one via caspase-8/Bid and the other via a caspase-8-independent pathway that possibly involves one or more kinases.

In death receptor-induced apoptosis, activation of Bak is mainly mediated by the caspase-8/Bid pathway. Because we showed that Fas-induced caspase-independent exposure of the N terminus of Bak occurred in MEFs in the absence of cycloheximide, which was suggested to overcome the inhibitory effect of cFLIP or vFLIP on death-inducing signaling complex-dependent activation of caspase-8 (40), the caspase-independent signaling pathway that primes Bak might contribute to some death paradigms such as elimination of cells infected with vFLIP-producing virus by cooperation with other intrinsic apoptotic signals targeting the mitochondria.

In conclusion, a death receptor-activated caspase-independent signal induces exposure of the N terminus of Bak. Although this change is not sufficient for activation, it primes Bak for full activation. Thus, our results have revealed a novel signaling pathway involved in death receptor-mediated apoptosis.

Acknowledgment—We are grateful to Dr. S. Nagata for providing a caspase-8-deficient derivative of Jurkat (JB6).

REFERENCES

1. Wolf, B. B., and Green, D. R. (2002) *Curr. Biol.* **12**, R177–R179
2. Wang, X. (2001) *Genes Dev.* **15**, 2922–2933
3. Tsujimoto, Y. (2003) *J. Cell. Physiol.* **195**, 158–167
4. Danial, N. N., and Korsmeyer, S. J. (2004) *Cell* **116**, 205–219
5. Wei, M. C., Zong, W. X., Cheng, E. H., Lindsten, T., Panoutsakopoulou, V., Ross, A. J., Roth, K. A., MacGregor, G. R., Thompson, C. B., and Korsmeyer, S. J. (2001) *Science* **292**, 727–730
6. Lindsten, T., Ross, A. J., King, A., Zong, W. X., Rathmell, J. C., Shiels, H. A., Ulrich, E., Waymire, K. G., Mahar, P., Frauwirth, K., Chen, Y., Wei, M., Eng, V. M., Adelman, D. M., Simon, M. C., Ma, A., Golden, J. A., Evan, G., Korsmeyer, S. J., MacGregor, G. R., and Thompson, C. B. (2000) *Mol. Cell* **6**, 1389–1399
7. Scaffidi, C., Fulda, S., Srinivasan, A., Friesen, C., Li, F., Tomaselli, K. J., Debatin, K. M., Krammer, P. H., and Peter, M. E. (1998) *EMBO J.* **17**, 1675–1687
8. Luo, X., Budihardjo, I., Zou, H., Slaughter, C., and Wang, X. (1998) *Cell* **94**, 481–490
9. Li, H., Zhu, H., Xu, C. J., and Yuan, J. (1998) *Cell* **94**, 491–501
10. Desagher, S., Osen-Sand, A., Nichols, A., Eskes, R., Montessuit, S., Lauper, S., Maundrell, K., Antonsson, B., and Martinou, J. C. (1999) *J. Cell Biol.* **144**, 891–901
11. Wei, M. C., Lindsten, T., Mootha, V. K., Weiler, S., Gross, A., Ashiya, M., Thompson, C. B., and Korsmeyer, S. J. (2000) *Genes Dev.* **14**, 2060–2071
12. Eskes, R., Desagher, S., Antonsson, B., and Martinou, J. C. (2000) *Mol. Cell. Biol.* **20**, 929–935
13. Griffiths, G. J., Dubrez, L., Morgan, C. P., Jones, N. A., Whitehouse, J., Corfe, B. M., Dive, C., and Hickman, J. A. (1999) *J. Cell Biol.* **144**, 903–914
14. Hsu, Y. T., and Youle, R. J. (1998) *J. Biol. Chem.* **273**, 10777–10783
15. Antonsson, B., Montessuit, S., Sanchez, B., and Martinou, J. C. (2001) *J. Biol. Chem.* **276**, 11615–11623
16. Goping, I. S., Gross, A., Lavoie, J. N., Nguyen, M., Jemmerson, R., Roth, K., Korsmeyer, S. J., and Shore, G. C. (1998) *J. Cell Biol.* **143**, 207–215
17. Wolter, K. G., Hsu, Y. T., Smith, C. L., Nechushtan, A., Xi, X. G., and Youle, R. J. (1997) *J. Cell Biol.* **139**, 1281–1292
18. Cheng, E. H., Sheiko, T. V., Fisher, J. K., Craigen, W. J., and Korsmeyer, S. J. (2003) *Science* **301**, 513–517
19. Griffiths, G. J., Corfe, B. M., Savory, P., Leech, S., Esposti, M. D., Hickman, J. A., and Dive, C. (2001) *Oncogene* **20**, 7668–7676
20. Gross, A., Jockel, J., Wei, M. C., and Korsmeyer, S. J. (1998) *EMBO J.* **17**, 3878–3885
21. Antonsson, B., Montessuit, S., Lauper, S., Eskes, R., and Martinou, J. C. (2000) *Biochem. J.* **345**, 271–278
22. Shimizu, S., and Tsujimoto, Y. (2000) *Proc. Natl. Acad. Sci. U. S. A.* **97**, 577–582
23. Kawahara, A., Ohsawa, Y., Matsumura, H., Uchiyama, Y., and Nagata, S. (1998) *J. Cell Biol.* **143**, 1353–1360
24. Nomura, M., Shimizu, S., Ito, T., Narita, M., Matsuda, H., and Tsujimoto, Y. (1999) *Cancer Res.* **59**, 5542–5548
25. Shimizu, S., Eguchi, Y., Kamiike, W., Funahashi, Y., Mignon, A., Lacronique, V., Matsuda, H., and Tsujimoto, Y. (1998) *Proc. Natl. Acad. Sci. U. S. A.* **95**, 1455–1459
26. Mikhailov, V., Mikhailova, M., Pulkrabek, D. J., Dong, Z., Venkatachalam, M. A., and Saikumar, P. (2001) *J. Biol. Chem.* **276**, 18361–18374
27. Ruffolo, S. C., and Shore, G. C. (2003) *J. Biol. Chem.* **278**, 25039–25045
28. Cheng, E. H., Wei, M. C., Weiler, S., Flavell, R. A., Mak, T. W., Lindsten, T., and Korsmeyer, S. J. (2001) *Mol. Cell* **8**, 705–711
29. Varfolomeev, E. E., Schuchmann, M., Luria, V., Chiannilkulchai, N., Beckmann, J. S., Mett, I. L., Rebrikov, D., Brodianski, V. M., Kemper, O. C., Kollet, O., Lapidot, T., Soffer, D., Sobe, T., Avraham, K. B., Goncharov, T., Holtmann, H., Lonai, P., and Wallach, D. (1998) *Immunity* **9**, 267–276
30. Shinohara, H., Yagita, H., Ikawa, Y., and Oyaizu, N. (2000) *Cancer Res.* **60**, 1766–1772
31. Desbarats, J., Birge, R. B., Mimouni-Rongy, M., Weinstein, D. E., Palerme, J. S., and Newell, M. K. (2003) *Nat. Cell Biol.* **5**, 118–125
32. Lambert, C., Landau, A. M., and Desbarats, J. (2003) *Apoptosis* **8**, 551–562
33. Yang, X., Khosravi-Far, R., Chang, H. Y., and Baltimore, D. (1997) *Cell* **89**, 1067–1076
34. Eischen, C. M., Dick, C. J., and Leibson, P. J. (1994) *J. Immunol.* **153**, 1947–1954
35. Yin, X. M., Wang, K., Gross, A., Zhao, Y., Zinkel, S., Klocke, B., Roth, K. A., and Korsmeyer, S. J. (1999) *Nature* **400**, 886–891
36. Yethon, J. A., Epand, R. F., Leber, B., Epand, R. M., and Andrews, D. W. (2003) *J. Biol. Chem.* **278**, 48935–48941
37. Makin, G. W., Corfe, B. M., Griffiths, G. J., Thistlethwaite, A., Hickman, J. A., and Dive, C. (2001) *EMBO J.* **20**, 6306–6315
38. Kischkel, F. C., Lawrence, D. A., Tinel, A., LeBlanc, H., Virmani, A., Schow, P., Gazdar, A., Blenis, J., Arnott, D., and Ashkenazi, A. (2001) *J. Biol. Chem.* **276**, 46639–46646
39. Cifone, M. G., Roncaioli, P., De Maria, R., Camarda, G., Santoni, A., Ruberti, G., and Testi, R. (1995) *EMBO J.* **14**, 5859–5868
40. Krueger, A., Baumann, S., Krammer, P. H., and Kirchhoff, S. (2001) *Mol. Cell. Biol.* **21**, 8247–8254

THE JOURNAL OF BIOLOGICAL CHEMISTRY
Vol. 279, No. 41, Issue of October 8, pp. 42758–42764, 2004
Printed in U.S.A.

CA Repeats in the 3′-Untranslated Region of *bcl-2* mRNA Mediate Constitutive Decay of *bcl-2* mRNA* ♦

Received for publication, July 1, 2004
Published, JBC Papers in Press, August 3, 2004, DOI 10.1074/jbc.M407357200

Jung-Hee Lee‡, Mi-Hee Jeon‡, Yun-Jee Seo‡, Yong-Joon Lee‡, Jeong Heon Ko§, Yoshihide Tsujimoto¶, and Jeong-Hwa Lee‡‖

From the ‡Department of Biochemistry, The Catholic University of Korea, Seoul 137-701, Korea, the §Proteomics System Research Center, Korean Research Institute of Bioscience and Biotechnology, Daijeon 305-333, Korea, and the ¶Department of Post-genomics and Diseases, Osaka University Medical School and Solution Oriented Research for Sciences and Technology (SORST) of Japan Science & Technology Corporation (JST), Suita, Osaka 565-0871, Japan

An AU-rich element (ARE) in the 3′-untranslated region (UTR) of *bcl-2* mRNA has previously been shown to be responsible for destabilizing *bcl-2* mRNA during apoptosis through increasing AUF1 binding. In the present study, we investigated the effect of the region upstream of the ARE on *bcl-2* mRNA stability using serial deletion constructs of the 3′-UTR of *bcl-2*. Deletion of 30 nucleotides mostly consisting of the CA repeats, located upstream of the ARE, resulted in the stabilization of *bcl-2* mRNA abundance, in the absence or presence of the ARE. The specificity of the CA repeats in terms of destabilizing *bcl-2* mRNA was proven by the substituting the CA repeats with other alternative repeats of purine/pyriminine, but this had no effect on the stability of *bcl-2* mRNA. CA repeats alone, however, failed to confer instability to *bcl-2* or *gfp* reporter mRNAs, indicating a requirement for additional sequences in the upstream region of the 3′-UTR. Serial deletion and replacement of a part of the region upstream of the CA repeats revealed that the entire 131-nucleotide upstream region is an essential prerequisite for the CA repeat-dependent destabilization of *bcl-2* mRNA. Unlike the ARE, CA repeat-mediated degradation of *bcl-2* mRNA was not accelerated upon apoptotic stimulus. Moreover, the upstream sequences and CA repeats are conserved among mammals. Collectively, CA repeats contribute to the constitutive decay of *bcl-2* mRNA in the steady states, thereby maintaining appropriate *bcl-2* levels in mammalian cells.

Apoptosis is a tightly controlled cellular suicide program that is critical for the successful development of multicellular organisms, the maintenance of normal tissue homeostasis, and removal of damaged cells (1). The protooncogene *bcl-2*, originally isolated from the chromosomal breakpoint of a t(14, 18)-bearing B cell lymphoma, serves as an important repressor of apoptosis in a variety of cell types (2, 3). In line with its significant role in altering susceptibility to apoptosis, investigations of the mechanisms by which *bcl-2* expression is modulated may prove crucial for identifying therapeutic strategies for cancer and some neurodegenerative diseases and for defining the role of *bcl-2* in the development of multiple tissues (4).

Recent studies have indicated that *bcl-2* is regulated at both the transcriptional and posttranscriptional levels. A number of negative transcriptional regulatory sites have been described in the *bcl-2* promoter region (5, 6), and several transcription factors, including cAMP response element binding protein, A-Myb and WT1, are known to be involved in the positive regulation of *bcl-2* transcription (7–9). In addition to the promoter region, some sequences within the coding region, such as estrogen response elements, have also been demonstrated to mediate the transcriptional modulation of *bcl-2*, as was shown in breast cancer cell lines (10). The posttranscriptional modification of *bcl-2* includes the phosphorylation of Bcl-2 at the putative mitogen-activated protein kinase sites, which confers resistance against ubiquitination- and proteasome-dependent degradation (11, 12), and caspase-dependent cleavage, which results in the loss of anti-apoptotic activity (13, 14). Another mechanism of posttranscriptional regulation of *bcl-2* expression is based on mRNA stability. Recent reports have described that a conserved AU-rich element (ARE)[1] is present in the 3′-untranslated region (UTR) of *bcl-2* mRNA (15) and that interaction of ARE with a number of ARE-binding proteins, including AUF1, is associated with *bcl-2* mRNA decay during apoptosis (16, 17). In addition, transfection of a synthetic ribozyme targeting *bcl-2* ARE was shown to successfully down-regulate *bcl-2* mRNA expression accompanied by an increase in cell death in lymphoma cells (18), thus supporting the central role of ARE in the regulation of *bcl-2* gene expression.

A recent study using a cell-free *in vitro* degradation assay revealed that a 396-nt segment of the *bcl-2* 3′-UTR including the ARE was degraded faster than the ARE motif itself and that the 3′-UTR lacking the ARE was still degraded faster than control RNA (19). These findings suggest that, in addition to the ARE, other regulatory sites might exist in the 3′-UTR, upstream or downstream of the ARE. Here, we investigated the effect of the region upstream of the ARE on *bcl-2* mRNA stability and identified a new putative *bcl-2* mRNA destabilization determinant that contains CA repeats, mediating the constitutive decay of *bcl-2* mRNA.

EXPERIMENTAL PROCEDURES

Cell Culture and Transfection—The African green monkey kidney cells (COS7) were obtained from the American Type Culture Collection

* This work was supported by Grant R04-2002-000-00127-0 from the Basic Research Program of the Korea Science & Engineering Foundation. The costs of publication of this article were defrayed in part by the payment of page charges. This article must therefore be hereby marked "*advertisement*" in accordance with 18 U.S.C. Section 1734 solely to indicate this fact.

♦ This article was selected as a Paper of the Week.

‖ To whom correspondence should be addressed: Dept. Biochemistry, College of Medicine, The Catholic University of Korea, 505 Banpo-dong, Seocho-Gu, Seoul 137-701, Korea. Tel.: 82-2-590-1180; Fax: 82-2-596-4435; E-mail: leejh@catholic.ac.kr.

[1] The abbreviations used are: ARE, AU-rich element; 3′-UTR, 3′-untranslated region; CAR, CA-repeated region; Act D, actinomycin D; GFP, green fluorescence protein; DIG, digoxigenin; nt, nucleotide(s); GAPDH, glyceraldehyde-3-phosphate dehydrogenase; eNOS, endothelial nitric-oxide synthase.

and grown in Dulbecco's modified Eagle's medium supplemented with 10% heat-inactivated fetal bovine serum (Hyclone) and antibiotic solutions (100 units/ml penicillin and 100 μg/ml streptomycin, Invitrogen) under a 5% CO_2 humidified atmosphere at 37 °C. COS7 cells (1×10^5) were transfected in 6-well plates with 1 μg of plasmids using FuGENE 6 reagent (Roche Applied Science) according to the manufacturer's instructions. COS7 cells were harvested at 48 h after transfection for Northern and Western blotting. To evaluate mRNA degratation rates, further transcription was inhibited by adding actinomycin D (Act D) at 10 μg/ml (Sigma) 24 h after transfection, and then further incubating cells, before total RNA was extracted. To determine the degradation rate of *bcl-2* mRNA under apoptotic condition, 1 mM H_2O_2 was added to COS7 cells 1 h prior to treating Act D.

Plasmid Construction—A 1114-nt segment for the BU4 plasmid including the coding region (1459–2178) and 394 nt of the 3′-UTR was first obtained by PCR amplification using cDNA from HL60 cells as a template and corresponding primers flanked by an EcoRI restriction site (see Fig. 1A; all nucleotide positions were based on the sequence of accession number M13994 in GenBank™). The PCR products were purified from a 1% agarose gel and inserted into the TA cloning site of pGEM-T easy vector (Promega); sequences were confirmed by automated DNA sequencing. The EcoRI fragment was then subcloned in the EcoRI site of pCR3.1, named BU4. Other *bcl-2* cDNA constructs containing various lengths of the 3′-UTR were also produced by PCR using BU4 as a template for B, BU1, BU2, and BU3 and using BU3 for BU2-1, BU2-2, BU2-3, and BU2-4 with corresponding primers. For plasmids attached by other alternative repeats of purine and pyrimidine (BU2-2_{AT}, BU2-2_{CG}, BU2-2_{GT} and BU2-2_{CA}), reverse primers were designed to include five respective repeats at the last part, and BU2-2 was used as a template.

To prepare a chimeric cDNA, which contains a coding region of *bcl-2* and the 3′-UTR of unrelated gene followed by CA repeats ($BU3_{bis}$), two separate PCR amplifications were performed as follows. The first part confining the *bcl-2* coding region was synthesized with 5′-GAATTCATGGCGCACGCTGGGAGAACGGGG-3′ (forward, primer1) and 5′-GCTAGCTCACTTGTGGCTCAGATAGGCACC-3′ (reverse) flanked at the 5′-end by EcoRI and NheI restriction sites, respectively. The second part composed of 125 nt (1742–1866) in the 3′-UTR of the *bis* gene (GenBank™ accession number AF127139) and 30 nt of the CA-repeated region (CAR, 2310–2339) were PCR-amplified with forward primer 5′-GCTAGCCCTCTGCCCTGTAAAAATCAGACT-3′ and reverse primer 5′-GAATTCTGTGTGTGTGTGTCTGTCTGTGTGTGTGCACCCACGTTACTGC-3′ flanked at the 5′-end by NheI and EcoRI, respectively, using human *bis* gene (20) as a template. Each PCR product was independently cloned into pGEM-T easy vector and excised at the EcoRI and NheI sites for the first part and at the NheI and EcoRI sites for the second part. Two fragments were then ligated together into pCR3.1 at the EcoRI site to produce $BU3_{bis}$ construct in which 131 nt of the 3′-UTR of *bcl-2* was replaced with unrelated sequences including an NheI restriction site and part of the *bis* 3′-UTR. Two chimeric constructs of GFP, G2 and G3, were also prepared by ligating the two PCR products at the NheI and EcoRI sites as described above.

The 30 nt of CAR was directly inserted next to the stop codon (B_{CAR}) or following 42 nt ($B42_{CAR}$) or 82 nt ($B82_{CAR}$) of the 3′-UTR of *bcl-2* using 5′-GAATTCTGTGTGTGTGTGTCTGTCTGTGTGTGTGTCACTTGTGGCTCA-3′, 5′-GAATTCTGTGTGTGTGTGTCTGTCTGTGTGTGTGTAGTGAACCTT-3′, or 5′-GAATTCTGTGTGTGTGTGTCTGTCTGTGTGTGTGTATGGTACATC-3′ as reverse primers, respectively. The BU3-1, BU3-2, and BU3-3 constructs, in which a part of 131 nt in the 3′-UTR was replaced with unrelated sequences, were generated by ligating two PCR products using the XhoI site. The inserted sequence for the last 49 nt (BU3-3) is 5′-AATC<u>AGCAACTTCGTACCAGTAT(CTCGAG)ATCAGAACGTTGGAACTT</u>AT-3′ (the XhoI site is in parentheses). The underlined sequence was used to replace the first 42 nt (BU3-1) and the sequence in bold to replace for the middle 40 nt (BU3-2).

CAR was deleted from the 3′-UTR of BU4 plasmid ($BU4\Delta_{CAR}$) by a single step ligation of two the PCR products derived from BU4, upstream and down stream sequences of CAR, into the EcoRI sites of pCR3.1. Primer1 and 5′-<u>CTCGAG</u>GATGTTTATATGTGTGTTATTTTT-3′ containing a XhoI site (underlined) were used for the region upstream of CAR and 5′-CTCGAGCAATTAACAGTCTTCAGGCAAAAC-3′ with a XhoI site (underlined) and 5′-<u>GAATTC</u>GGTGATCCGGCCAACAAC-3′ with an EcoRI site (underlined) for the region downstream of CAR. Expression plasmids for mouse *bcl-2* were produced by PCR using cDNA from NIH3T3 cells and the primers corresponding to the various length of the 3′-UTR.

Northern Blot Analysis—Total RNA was extracted from cells using the RNAzol B reagent (Tel-Test Inc.), separated by electrophoresis through denaturing 2.2 M formaldehyde, 1% agarose gel, and then transferred onto positively charged nylon membrane by capillary blotting. Before blotting, 28 and 18 S ribosomal RNAs were visualized by ethidium bromide staining to ensure the integrity of the isolated RNA and to quantify RNA loading. RNA was UV cross-linked to the membrane, which was prehybridized for 1 h at 55 °C in high SDS hybridization buffer (5× SSC, 7% SDS, 50% formamide deionized, 0.1% *N*-lauroylsarcosine, 2% milk, and 50 mM sodium phosphate, pH 7.0), and then hybridized with digoxigenin (DIG)-labeled specified DNA probes, prepared by PCR labeling, in the same buffer at 55 °C overnight. The following primers were used to incorporate DIG-11 dUTP (Roche Applied Science) for different DNA probes; 5′-GGCAAGCTTGTGAACTGGGGGAGGATTGTG-3′ and 5′-GGCAAGCTTGAGCAGAGTCTTCAGAGACAG-3′ for *bcl-2*; 5′-TGAAGTTCATCTGCACCACC-3 and 5′-ACGAACTCCAGCAGGACCA-3 for GFP, and 5′-ACCACAGTCCATGCCATCAC-3′ and 5′-TCCACCACCCTGTTGCTGTA-3′ for GAPDH. The membrane was washed sequentially in 2× SSC, 0.1% SDS for 15 min at room temperature twice and in 0.1× SSC, 0.1% SDS for 15 min at 68 °C twice. Specific hybridization was then immunodetected with alkaline phosphatase-conjugated anti-DIG antibody (1:10,000, Roche Applied Science) followed by chemiluminescent substrate CDP-star (Roche Applied Science).

To determine the rate of *bcl-2* mRNA decay, total RNA was isolated from cells at multiple time points after treatment with Act D and then subjected to Northern blot analysis as described above. The membrane was stripped and rehybridized with GAPDH probe. The *bcl-2* mRNA signal was quantified at each time point by densitometry using Scion image software (Scion Corp.), normalized to GAPDH, and plotted as a percentage of the initial value against time.

Immunoblot Assay for Bcl-2 and Actin Proteins—Cells were lysed in RIPA buffer (50 mM Tris-HCl, pH 7.4, 150 mM sodium chloride, 1% Nonidet P-40, 0.5% sodium deoxycholate, 0.1% sodium dodecyl sulfate), and equal amounts of protein were separated by 12.5% SDS-PAGE followed by electrotransfer onto a polyvinylidene difluoride membrane (Milipore). The membranes were incubated with a monoclonal antibody to human Bcl-2 (Santa Cruz Biotechnology), GFP (Clontech), or β-actin (Sigma) and developed after incubation with horseradish peroxidase-conjugated secondary antibodies (Promega) using the enhanced detection system (Amersham Biosciences).

In Vitro Transcription—To examine the effect of the presence of the CA repeats in the 3′-UTR on the transcription of *bcl-2*, the transcripts of BU2 or BU3 constructs were synthesized *in vitro* using T7 RNA polymerase (21). BU2 or BU3 was first subcloned into the EcoRI site of pBluescript SK− in sense orientation with respect to the T7 promoter. *In vitro* transcripts were then synthesized using 0.5 μg of DNA linearized at the SpeI site with 20 units of T7 polymerase (Roche Applied Science) in transcription reaction buffer containing 20 units of RNase inhibitor and a 0.05 mM concentration each of ATP, CTP, GTP, and UTP for 2 h at 37 °C according to the manufacturer's instruction. After treatment of DNase I (Promega, 1 unit/reaction), the purity as well as the amount of RNA transcripts were determined by using 1% formaldehyde-agarose gel followed by ethidium bromide staining.

RESULTS

The CA Repeats in the 3′-UTR Contribute to the Destabilization of bcl-2 mRNA—To investigate the contribution of the sequence of the 3′-UTR upstream of the ARE of *bcl-2* to the stability of *bcl-2* mRNA, we prepared a series of 3′-UTR deletion mutants of *bcl-2* between its stop codon and the ARE by PCR, as shown in Fig. 1A. Each cDNA fragment-containing coding region and the indicated portion of the 3′-UTR was inserted into the pCR3.1 vector. The resulting constructs were transiently transfected into COS7 cells, and the level of *bcl-2* expression from each construct was analyzed by Northern and Western blotting. Fig. 1*B* shows that no significant differences of *bcl-2* expression were found in cells transfected with B, BU1, or BU2. However, the *bcl-2* mRNA level was lower in cells transfected with the BU3 cDNA than in cells transfected with B, BU1, or BU2 but was higher than in cells transfected with BU4 cDNA, which includes the ARE previously reported to be an apoptosis-dependent destabilizing element for *bcl-2* mRNA (15). Similar results were obtained in Western blotting assays of Bcl-2 protein expression levels (Fig. 1*B*). Since all constructs used in this experiment were cloned into the same pCR3.1

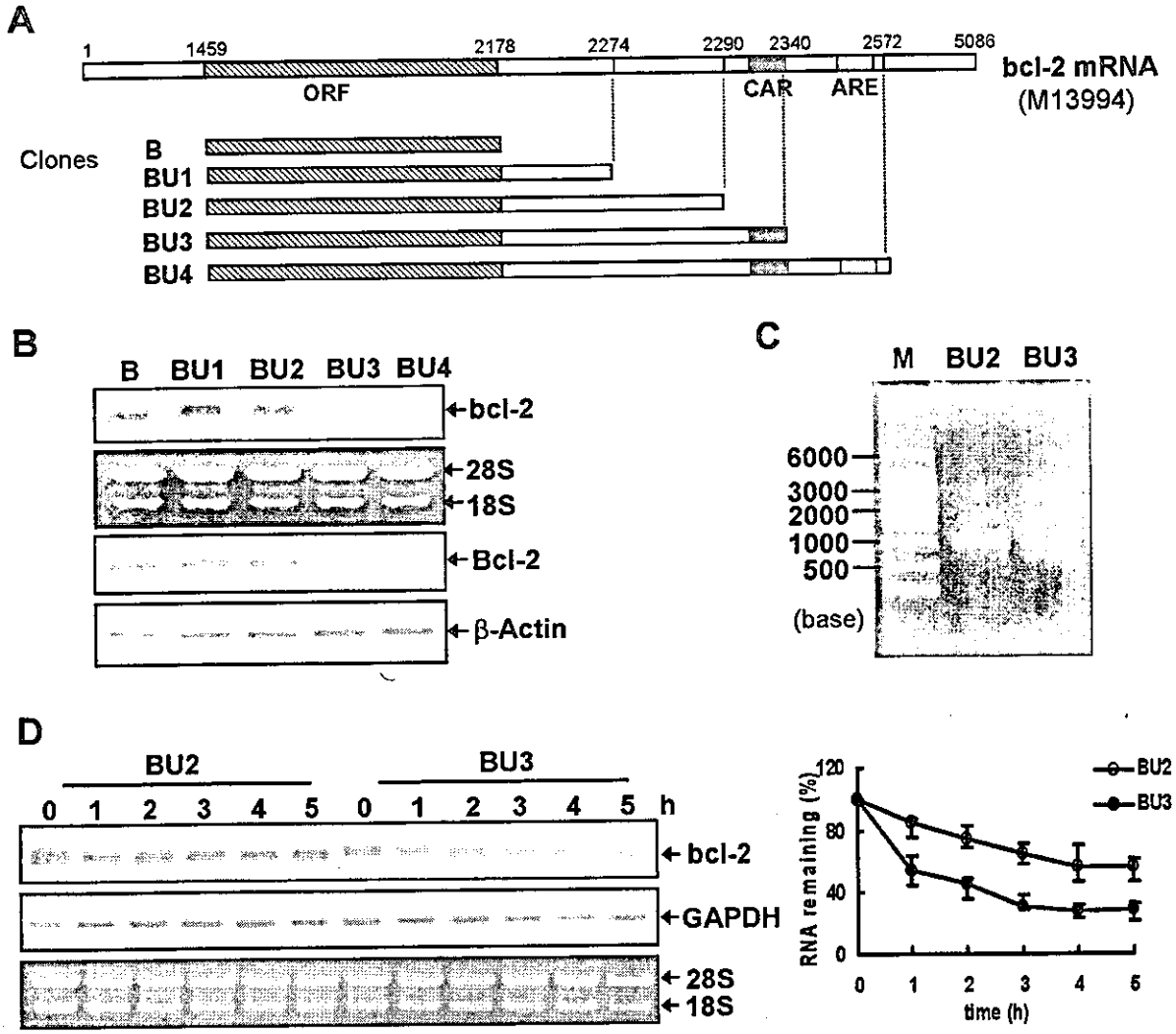

FIG. 1. **Regulation of *bcl-2* mRNA stability by a region upstream of ARE in the 3′-UTR.** *A*, schematic representation of five *bcl-2* constructs, which include various lengths of the 3′-UTR. The open reading frame (1459–2178) is shown as a *box* with *dashed lines*, and the previously reported ARE (2371–2465) is represented by a *gray box*. The *black box* indicates the CAR. The nucleotide sequence shown is based on the GenBank™ data base under accession number M13994. *B*, expression of *bcl-2* mRNA and Bcl-2 protein derived from various constructs shown in *A*. COS7 cells were transiently transfected with 1 μg of each constructs, and total RNA and protein were extracted after 48 h of transfection. Northern blot analysis was performed using 3 μg of total RNA using DIG-labeled *bcl-2* probe. Ethidium bromide-stained 28 and 18 S ribosomal RNAs were used as loading controls. Western blot analysis was performed in parallel with Northern blotting. One μg of the total protein was separated by 12.5% SDS-PAGE, transferred to a membrane, and probed with an anti-Bcl-2 monoclonal antibody followed by a β-actin antibody. *C*, *in vitro* transcription of the coding region and subsequent region of the 3′-UTR of BU2 and BU3 was performed as described under "Experimental Procedure." RNA was visualized by staining with ethidium bromide. *D*, comparison of *bcl-2* mRNA degradation mediated by 3′-UTR of BU2 and BU3 constructs. mRNA decay rates were determined by Act D chase experiments and Northern blotting. 24 h after transfection, 10 μg/ml Act D was added to COS7 cells, which were harvested at the indicated times for hybridization with the *bcl-2* probe, and subsequently with a GAPDH probe as a loading control (*left panel*). *bcl-2* mRNA remaining at each time point was plotted against time as a percentage of its initial value, after being normalized to GAPDH (*right graph*). Signal intensity at time 0 was defined as 100%. Results are shown as means ± of S.D. of three independent experiments.

vector, which has a cytomegalovirus promoter, the difference in the *bcl-2* mRNA level between BU2 and BU3 constructs was likely to be due to the differences in mRNA stability rather than differences in the transcription rate. Supporting our presumption, *in vitro* transcription experiments using T7 polymerase and BU2 or BU3 as templates revealed no significant difference in transcript level from each template (Fig. 1*C*).

We then compared the mRNA degradation rates of the transcripts from these two constructs by Act D chase experiments. Fig. 1*D* shows that the mRNA level of BU3 was reduced to 29% of the control at 5 h after adding Act D, while the mRNA level of BU2 was maintained at 56% of the control level, indicating that the BU3 mRNA was degraded faster than the BU2 mRNA. Therefore, these results suggest that the part of the 3′-UTR region present in BU3 but deleted in BU2 has the potential to affect *bcl-2* mRNA stability rather than the transcription processes.

To identify in detail the sequences with the mRNA destabilizing potential, the last 50 nt of the 3′-UTR sequences of the BU3 cDNA were serially deleted in 10-nt increments, and the expression levels of each construct were then compared by Northern blotting. As shown in Fig. 2*B*, transfection of the BU2-1 or BU2-2 construct, which, respectively, has 10 or 20 bases more than the BU2 construct, did not cause any decrease in the *bcl-2* mRNA level compared with BU2 cDNA. However, the mRNA level gradually decreased in the cells transfected with BU2-3, BU2-4, or BU3, which had serial additions of 10 nt, up to 30 nt. Interestingly, the sequences of these 30 nt (2311–2340), which dramatically reduced the *bcl-2* mRNA level, are mostly composed of CA repeats (+2 GA), indicating

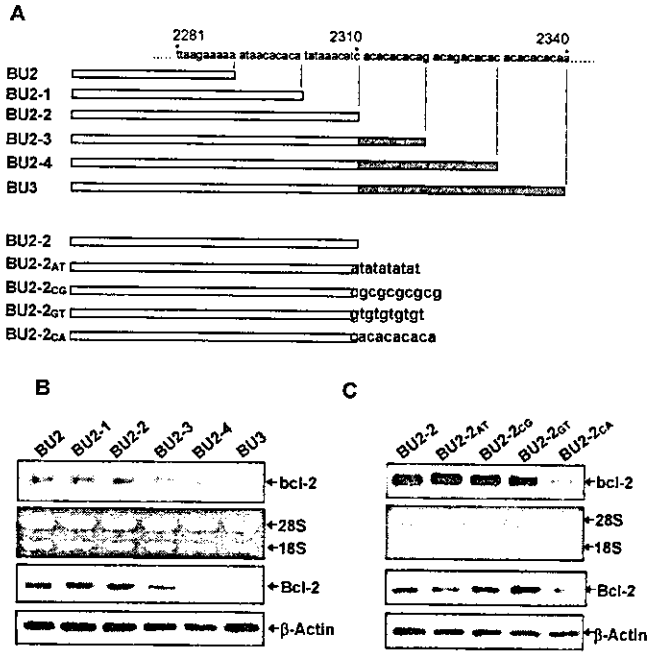

FIG. 2. **The *bcl-2* mRNA stability is regulated by CA repeats in the 3′-UTR.** *A*, schematic representation of the 3′-UTR of several *bcl-2* constructs. The coding region is not shown for convenience. The *upper panel* represents deletion mutants of 3′-UTR in which 10 nt were serially deleted from the 3′-end of the BU3 construct. The *lower panel* shows that five repeats of CA of BU2-3 were substituted with other purine-pyrimidine repeated sequences. *B* and *C*, Northern and Western blottings of *bcl-2* mRNA and protein, respectively, from deletion constructs, BU2, BU2-1, BU2-2, BU2-3, BU2-4, and BU3 (*B*) and from BU2-2, BU2-2_{AT}, BU2-2_{CG}, BU2-2_{GT}, and BU2-2_{CA} (*C*). Transfection and detection were performed as described in the legend to Fig. 1.

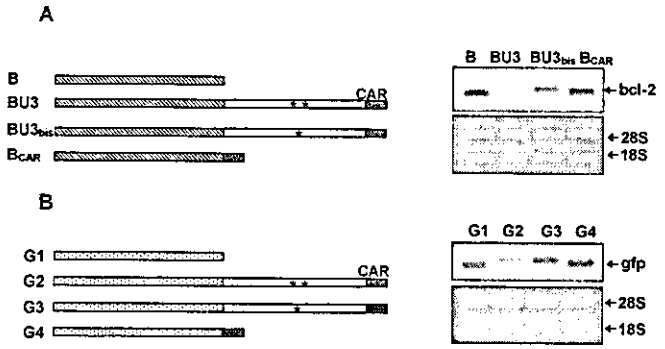

FIG. 3. **CA repeats are required but not sufficient for destabilization of *bcl-2* mRNA.** Schematic diagrams of *bcl-2* constructs (*A*) and GFP constructs (*B*) are shown in the *left panel* and the mRNA expressions of these constructs in the *right panel*. The coding region of the *bcl-2* and GFP genes are presented as *dashed* and *dotted boxes*, respectively. The $BU3_{bis}$ and G3 constructs include the 3′-UTR of the *bis* gene (*) and the CAR of the *bcl-2* gene, and G2 includes 131 nt of the 3′-UTR of the *bcl-2* gene (**), which was attached to the coding region of GFP. In B_{CAR} and G4 constructs, 30 nt of CA repeats was directly inserted into the 3′-end of the coding regions of *bcl-2* and GFP, respectively. Transfection and Northern blotting were carried out as described in the legend to Fig. 1.

that *bcl-2* mRNA stability decreased in proportion to the length of the CA repeats. We designated this region as CAR. It is notable that the BU2-3 construct, which has only five CA repeats, significantly reduced the *bcl-2* mRNA level. When the five repeats of CA in the BU2-3 cDNA were replaced with five repeats of AT, CG, or GT, as shown in Fig. 2*C*, the mRNA levels derived from these three constructs were similar to the mRNA level of the BU2-2 construct without the CA repeats, excluding the possibility that a simple repeat of purine and pyrimidine rather than sequence-specific CA repeats affect *bcl-2* mRNA stability.

Sequences Upstream of the 3′-UTR Are Required for CA Repeat-dependent Destabilization of bcl-2 mRNA—To establish whether the presence of CA repeats alone is sufficient to regulate *bcl-2* mRNA stability, we made two chimeric constructs, termed $BU3_{bis}$ and B_{CAR}, respectively, as indicated in Fig. 3*A*. Transfection with the B_{CAR} construct, in which 131 nt of the *bcl-2* 3′-UTR upstream of CA repeats were deleted, resulted in a marked stabilization of *bcl-2* mRNA despite the presence of the CA repeats, indicating an additional requirement of the proximal sequences of 3′-UTR for the CA repeat-dependent destabilization of *bcl-2* mRNA. Replacement of the proximal 131 nt of the *bcl-2* 3′-UTR with the unrelated sequences of 131 nt of the *bis* 3′-UTR also failed to destabilize *bcl-2* mRNA as efficiently as the 3′-UTR of *bcl-2*, even though a slight destabilization was observed. Therefore, it is not the simple distance between the stop codon and the CA repeats but the specific sequences in the 131 nt of the 3′-UTR that seem to confer the destabilizing potential of the CA repeats.

The destabilizing activity of the proximal region of the 3′-UTR of *bcl-2* was confirmed using a GFP reporter gene. The 3′-end of the open reading frame of the GFP cDNA was linked to the 131 nt of the 3′-UTR of *bcl-2* and subsequently to 30 nt of CA repeats, or directly to the CA repeats only, as described under "Experimental Procedures." Compared with the mRNA level expressed from the GFP coding region only, the insertion of 131 nt of the 3′-UTR together with CA repeats into the GFP coding region resulted in a comparable decrease in the GFP mRNA level, whereas insertion of the CA repeats only caused no decrease (Fig. 3*B*). The incorporation of 131 nt of the 3′-UTR of the *bis* gene, instead of the 3′-UTR of *bcl-2*, had no effect on *gfp* mRNA stability as in *bcl-2* mRNA, verifying the potential destabilizing activity of the 3′-UTR of *bcl-2*, which demands both the proximal 3′-UTR of *bcl-2* and subsequent CA repeats.

To determine the essential region affecting the CA repeat-dependent *bcl-2* mRNA destabilization, we attached 30 nt of CA repeats to 42 or 82 nt of the 3′-UTR of *bcl-2*. The *bcl-2* mRNA expressed from these two chimeric constructs showed significantly high levels, which corresponded to the mRNA levels from the construct in which all 131 nt were deleted (Fig. 4*A*). These results suggest that the last part of the 131 nt, lacking in these two constructs but present in the BU3 wild type, might be important for the CA repeat-dependent destabilization of *bcl-2* mRNA.

Subsequently, the last part of the proximal 131 nt of the 3′-UTR, as well as the first and middle part, were substituted with unrelated sequences. As shown in Fig. 4*B*, the replacement of each part increased *bcl-2* mRNA stability to a level similar to that of construct B, which contains only the coding region (Fig. 4*B*). These results, taken together, indicated that the overall mRNA structure provided by the linear sequences of the complete 131 nt of the 3′-UTR might be a prerequisite for the destabilizing ability of the subsequent CA repeats.

CA Repeat-dependent bcl-2 mRNA Destabilization Is Not Affected by Apoptosis—It has been reported previously that ARE-mediated decay in *bcl-2* mRNA is enhanced during apoptosis and that this is accompanied by increased binding of several AUBFs (15–17). To determine whether CA repeat-mediated *bcl-2* mRNA degradation also participates in the down-modulation of Bcl-2 during apoptosis, we investigated whether the degradation rate of *bcl-2* mRNAs with the 3′-UTR including the CA repeats but lacking ARE is affected by apoptotic stimulation. Act D chase experiments up to 5 h following transient transfection for 24 h revealed that the degradation of *bcl-2* mRNA with both CA repeats and ARE (BU4) was significantly accelerated by H_2O_2 treatment (Fig. 5, *B* and *central panel* of

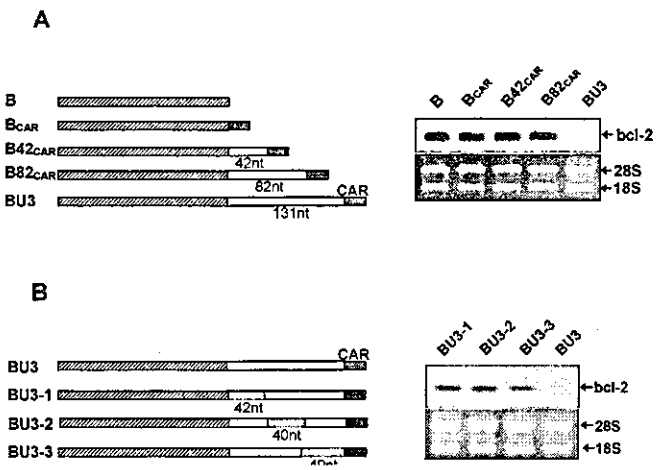

FIG. 4. **CA repeat-dependent destabilization of *bcl-2* mRNA requires sequences upstream of the CA repeats.** The upstream region to CA repeats was sequentially deleted (*A*) or replaced in part by unrelated sequences (*B*) as shown in the *left panel*. *Gray boxes* represent the substituted regions. The constructs were transfected into COS7 cells and Northern blotting was performed. 18 and 28 S were stained with ethidium bromide as RNA loading controls.

C), which is consistent with the earlier observation (15). However, the *bcl-2* mRNA with the CA repeats but lacking the ARE (BU3) was degraded at similar rates in the absence or presence of H_2O_2 to 38 or 33%, respectively, after treatment with Act D for 5 h, indicating that apoptotic conditions did not influence *bcl-2* mRNA decay mediated by CA repeats (Fig. 5, *B* and *left panel* of *C*). We also examined the decay of *bcl-2* mRNA with the ARE but not the CA repeats ($BU4\Delta_{CAR}$). Deletion of the CA repeats led to marked stabilization of *bcl-2* mRNA levels in the steady state, despite the presence of the ARE, but greatly enhanced the degradation of *bcl-2* mRNA following H_2O_2 treatment, as was revealed by a reduction in the remaining RNA from 107% to 35% after 5 h of Act D treatment (Fig. 5, *B* and *right panel* of *C*). These results, taken together, indicated that the degradation of *bcl-2* mRNA under apoptotic conditions was mainly mediated through the ARE component and that the CA repeats in the 3′-UTR may contribute to the constitutive decay of *bcl-2* mRNA.

Effect of CA Repeats on Mouse bcl-2 mRNA Stability—Whereas the ARE in the 3′-UTR of the *bcl-2* gene has been reported to be highly conserved in the human, mouse, chicken, and nematode (15), the CA repeats are confined to the 3′-UTRs of mammalian *bcl-2* genes. CA repeats in mouse *bcl-2*, located 115 nt from the stop codon, include 23 repeats of CA without G, and the sequences upstream of the CA repeats share 79% of homology with those of human *bcl-2* (Fig. 6*A*). To investigate whether CA repeats present in the 3′-UTR of the *bcl-2* genes of other species also exert destabilizing activity on its mRNA, we compared the mouse *bcl-2* mRNA levels from three different constructs. The mouse *bcl-2* gene with only coding sequences expressed a higher level of *bcl-2* mRNA compared with the mouse *bcl-2* mRNA with 161 nt of the 3′-UTR including the CA repeats. In addition, a 46-nt deletion of the CA repeats resulted in the marked stabilization of *mbcl-2* mRNA (Fig. 6*B*), as seen in human *bcl-2* mRNA. Therefore, the mRNA destabilizing ability of CA repeats in the 3′-UTR of *bcl-2* appears to be preserved among mammals to maintain *bcl-2* mRNA levels in various cellular environments.

DISCUSSION

ARE-mediated mRNA decay has recently been implicated in the regulation of *bcl-2* mRNA stability, which is activated by an apoptotic program (15–17). In this study we found that *bcl-2* mRNA decay is also modulated in part by the CA repeats in the 3′-UTR, which are located about 131 nt from the stop codon and upstream of the previously characterized ARE. The destabilizing potential of the CA repeats was confirmed by deleting the CA repeats from the 3′-UTR of *bcl-2*, which resulted in a marked increase in the level of *bcl-2* mRNA despite the presence of the ARE sequence (Fig. 5). These results suggest that the CA repeat is a novel determinant of *bcl-2* mRNA decay, which is in line with the previous finding that an ARE-deficient 3′-UTR of *bcl-2* was still degraded faster than control 3′-UTR *in vitro*, suggesting the presence of an additional *bcl-2* mRNA decay-regulatory element in the 3′-UTR (19). Therefore, the destabilizing activity of the 3′-UTR of *bcl-2* including the ARE demonstrated in earlier studies, which primarily focused on the ARE as a representative *bcl-2* mRNA destabilizing determinant, seems to be attributable not entirely to the ARE but substantially to CA repeats as well.

CA repeats are the most common dinucleotide polymorphism found in the human genome and thus are routinely used as genetic markers of allelic variants in various genes (22–24). Recently, a number of reports have described a correlation between the reduced expression levels of several genes such as IFN-γ and HSD11B2 and either the presence of repeats or an increase in the length of the repeats in the intron, suggesting a regulatory function of CA repeats on the processing of pre-mRNAs (25–27). Furthermore, CA repeats in intron 13 of the human endothelial nitric-oxide synthase (eNOS) gene seem to specify the cleavage site of the pre-mRNA of eNOS for splicing or degradation, depending on the presence of heterogeneous nuclear ribonucleoprotein L (hnRNPL) (28, 29). However, little is known about the functional importance of CA repeats in the exonic context. Here we describe for the first time that CA repeats in the 3′-UTR can target *bcl-2* mRNA for selective degradation, extending the role of CA repeats as an important element for modulating the stability of mRNA as well as the stability of pre-mRNA.

The mechanism by which CA repeats in an exon exert a negative effect on *bcl-2* mRNA abundance has not been clarified. However, exonic CA repeats for mRNA destabilization appear to involve a different pathway from that of intronic CA repeats for specifying the cleavage sites of the pre-RNA of eNOS, given that the CA repeats did not function as a splicing enhancer when moved in an exonic context (28). Furthermore, CA repeats were shown to be sufficient for the cleavage of eNOS pre-mRNA (29), whereas CA repeats were found to be essential but not sufficient to destabilize *bcl-2* mRNA, as shown by our results indicating that the incorporation of the CA repeats directly into the 3′-end of coding sequences of *bcl-2* or GFP mRNA did not affect mRNA stability (Fig. 3, *A* and *B*). On the other hand, levels of GFP reporter gene mRNA decreased after introduction of the proximal 131 nt and subsequent CA repeats of the 3′-UTR of *bcl-2*, whereas the incorporation of the same length of the 3′-UTR of the *bis* gene with the CA repeats had no effect on GFP or *bcl-2* mRNA stability. Finally, our deletion and replacement experiments indicate that the entire 131 nt region preceding the CA repeats is apparently a requisite for the destabilizing activity of the CA repeats (Fig. 4, *A* and *B*).

In addition to the requirement of the upstream sequences of the 3′-UTR, CA repeat-mediated decay of *bcl-2* mRNA was found to exhibit features that differed from ARE-mediated processes in several respects. The ARE in the 3′-UTR of *bcl-2* has been known to mediate *bcl-2* mRNA decay during apoptosis, either by increasing binding of destabilizing factors such as AUF1 (16, 17) or by reducing interaction with stabilizing factors such as nucleolin (30, 31). Our results show that the decay

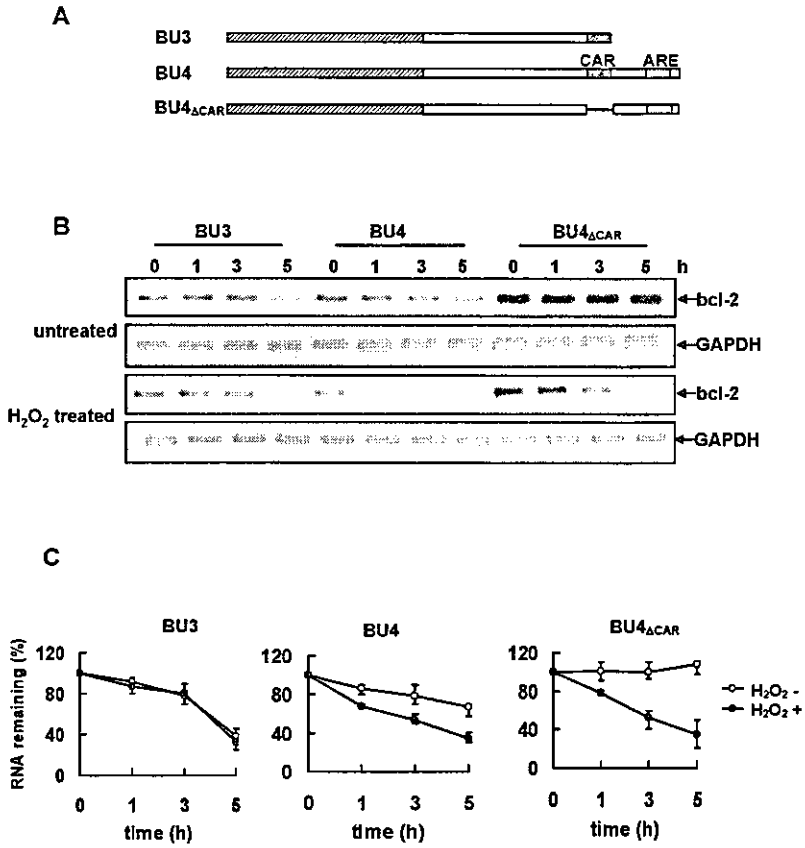

FIG. 5. **CA repeat-dependent decay of *bcl-2* mRNA is not enhanced by apoptosis.** COS7 cells were transiently transfected with three *bcl-2* constructs including CAR (BU3), ARE only (BU4Δ_{CAR}), or both (BU4) in the 3′-UTR as shown in *A*, and *bcl-2* mRNA stability was analyzed in the presence of Act D. To induce apoptosis, H_2O_2 (1 mM) was added to cells 1 h prior to adding Act D (10 μg/ml). Total RNA was extracted at 0, 1, 3, or 5 h after Act D treatment and analyzed by Northern blot for *bcl-2* and subsequently for GAPDH as shown in *B*. *C*, *bcl-2* mRNA signals derived from the three constructs (BU3, BU4, and BU4Δ_{CAR}) under normal and apoptotic condition were normalized with GAPDH mRNA signal from each lane in *B* after being quantified by densitometry using Scion image software (Scion Corp.). All data are represented as means ± S.D. from three independent experiments. *bcl-2* mRNA signal without Act D was defined as 100% and Act D-treated *bcl-2* mRNA levels were calculated as percentages of decay at the indicated times.

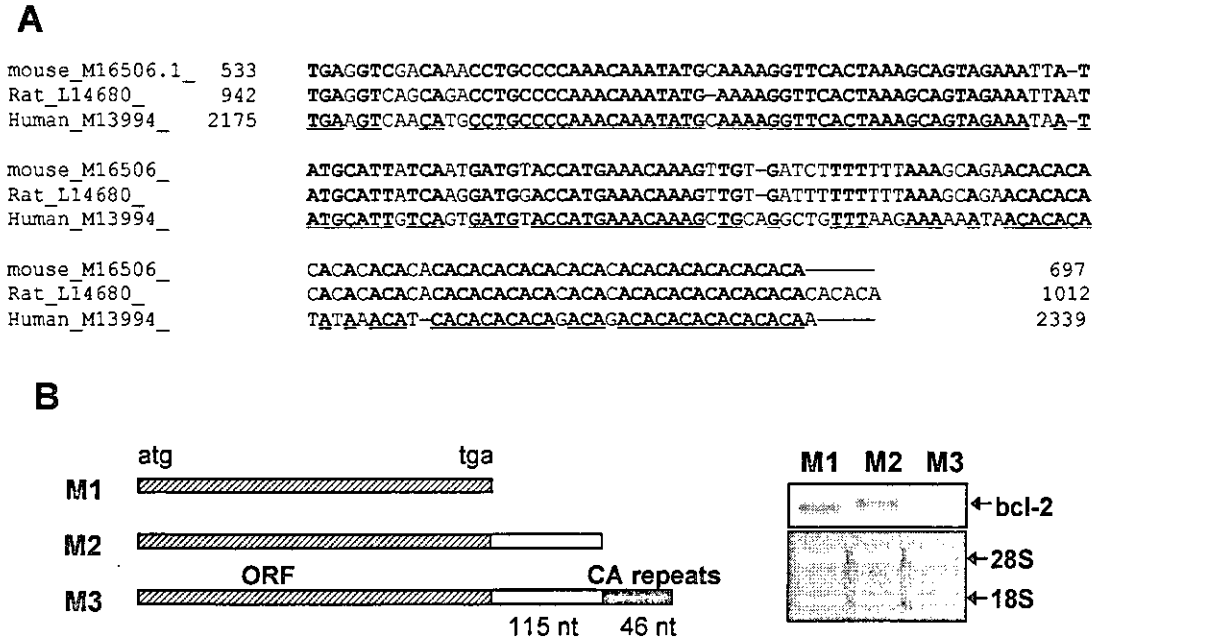

FIG. 6. **The nucleotide sequences and destabilization potential of an upstream portion of the 3′-UTR and CA repeats of the *bcl-2* gene are conserved in mammals.** *A*, the nucleotide sequences of the region upstream of the CA repeats in the 3′-UTR of *bcl-2* gene were compared for human, rat, and mouse (GenBank™ accession numbers on the *left*). Alignment was performed starting from the first nucleotide of the stop codon up to the last nucleotide of the CA repeats. The shared nucleotides among these three species are in *bold* and *underlined*. Multiple alignment comparison was performed using the ClustalW engine (www.justbio.com/aligner/). *B*, three constructs of mouse *bcl-2*, prepared as shown in the *left panel*, were transfected into COS7 cells, and *bcl-2* mRNA levels were analyzed (*right panel*).

rate of the *bcl-2* mRNA from the construct including the CA repeats but not the ARE was not significantly changed upon apoptosis induction, whereas *bcl-2* mRNA from the construct including the ARE and CA repeats was degraded faster under the same conditions (Fig. 5). Moreover, the transcript from the *bcl-2* DNA including the ARE but devoid of the CA repeats showed increased stability in nonapoptotic conditions but accelerated degradation in apoptotic conditions. Therefore, CA repeat-mediated decay of *bcl-2* appears to contribute to maintaining appropriate Bcl-2 levels in the steady states, while the ARE-dependent destabilizing pathway may react to apoptotic stimuli to permit a rapid down-regulation of the Bcl-2 level,

thereby leading to cell death. However, more diverse apoptotic stimuli should be applied to confirm the relevance of these two cis-elements in Bcl-2 down-regulation in apoptosis. Interestingly, the presence of Bcl-2 protein was previously proposed as an essential requirement for the activation of ARE-dependent degradation programs (19). We also found that the destabilizing effect induced by the incorporation of the upstream sequences and CA repeats of the 3′-UTR of *bcl-2* on GFP mRNA was less prominent than that of *bcl-2* mRNA (Fig. 3), raising the possibility that CA repeat-mediated decay also entails the presence of Bcl-2 protein. However, the coexpression of Bcl-2 did not influence the level of GFP mRNA with or without the 3′-UTR of the *bcl-2* gene in our study (data not shown). The amount of Bcl-2 protein was therefore not likely to be a critical prerequisite for the CA repeat-mediated decay of *bcl-2* mRNA, but another cis-element in the coding region of *bcl-2* might participate in the maintenance of the steady-state level of *bcl-2* mRNA. Another difference is that the presence of CA repeats in the 3′-UTR of *bcl-2* is confined to mammals, including humans, rats, and mice, whereas ARE is widely preserved, even being present in the 3′-UTR of nematode *bcl-2* (15). Moreover, the sequences 5′-upstream of the CA repeats also reveal a high level of homology in mammalian *bcl-2* (Fig. 6). Thus, CA repeat-mediated decay systems might have developed during evolutionary division into mammals to tune the *bcl-2* level more finely. The presence of diverse modes of regulating the Bcl-2 level, as shown in our report and in previous reports (15–17), suggests that different mechanisms are involved in the modulation of the Bcl-2 level in response to different physiological and pathological conditions.

Most of the mechanisms that regulate mRNA stability involve specific interactions between structural determinants on mRNA, cis-acting elements and proteins that bind the determinants, trans-acting proteins, which modulate the susceptibility of mRNA to degradation (32). Cis-acting elements could be an actual target site for ribonuclease, or they might regulate ribonuclease attack elsewhere in the mRNA by binding with either stabilizing or destabilizing factors. It has been shown previously that CA repeats or CA-rich sequences have the potential to bind proteins such as heterogeneous nuclear ribonucleoprotein (hnRNP) in the intron of eNOS pre-mRNA or in the 3′-UTR of vascular endothelial growth factor (VEGF) mRNA (28, 33). Therefore, defining whether a protein binds to the upstream sequences or CA repeats in the 3′-UTR of *bcl-2* and subsequently affects the *bcl-2* mRNA stability will be a subject of further investigation to get a complete understanding of the process of destabilizing *bcl-2* mRNA.

In conclusion, we describe a novel pathway of constitutive decay of *bcl-2* mRNA that involves CA repeats and their upstream sequences in the 3′-UTR, extending the functional significance of CA repeats from an intronic to an exonic context. Further investigation on the molecular mechanisms by which the CA repeats exert their destabilizing activity, including RNA/protein interactions, may contribute to the development of new strategies for reducing Bcl-2 levels in pathological conditions.

REFERENCES

1. Steller, H. (1995) *Science* **267,** 1445–1449
2. Tsujimoto, Y., Yunis, J., Onorato-Showe, L., Erikson, J., Nowell, P. C., and Croce, C. M. (1984) *Science* **224,** 1403–1406
3. Tsujimoto, Y., and Shimizu, S. (2000) *FEBS Lett.* **466,** 6–10
4. Bettaieb, A., Dubrez-Daloz, L., Launay, S., Plenchette, S., Rebe, C., Cathelin, S., and Solary, E. (2003) *Curr. Med. Chem. Anti-Canc. Agents* **3,** 307–318
5. Young, R. L., and Korsmeyer, S. J. (1993) *Mol. Cell. Biol.* **13,** 3686–3697
6. Miyashita, T., Harigai, M., Hanada, M., and Reed, J. C. (1994) *Cancer Res.* **54,** 3131–3135
7. Mayo, M. W., Wang, C-Y., Drouin, S. S., Madrid, L. V., Marshall, A. F., Reed, J. C., Weissman, B. E., and Baldwin, A. S. (1999) *EMBO J.* **18,** 3990–4003
8. Pugazhenthi, S., Miller, E., Sable, C., Young, P., Heidenreich, K. A., Boxer, L. M., and Reusch, J. E.-B. (1999) *J. Biol. Chem.* **274,** 27529–27535
9. Heckman, C. A., Mehew, J. W., Ying, G-G., Introna, M., Golay, J., and Boxer, L. M. (2000) *J. Biol. Chem.* **275,** 6499–6508
10. Perillo, B., Sasso, A., Abbondanza, C., and Palumbo, G. (2000) *Mol. Cell. Biol.* **20,** 2890–2901
11. Dimmeler, S., Breitschopf, K., Haendeler, J., and Zeiher, A. M. (1999) *J. Exp. Med.* **189,** 1815–1822
12. Breitschopf, K., Haendeler, J., Malchow, P., Zeiher, A. M., and Dimmeler, S. (2000) *Mol. Cell. Biol.* **20,** 1886–1896
13. Cheng, E. H., Kirsch, D. G., Clem, R. J., Ravi, R., Kastan, M. B., Bedi, A., Ueno, K., and Hardwick, J. M. (1997) *Science* **278,** 1966–1968
14. Del Bello, B., Valentini, M. A., Zunino, F., Comporti, M., and Maellaro, E. (2000) *Oncogene* **20,** 4591–4595
15. Schiavone, N., Rosini, P., Quattrone, A., Donnini, M., Lapucci, A., Citti, L., Bevilacqua, A., Nicolin, A., and Capaccioli, S. (2000) *FASEB J.* **14,** 174–184
16. Donnini, M., Lapucci, A., Papucci, L., Witort, E., Tempestini, A., Brewer, G., Bevilacqua, A., Nicolin, A., Capaccioli, S., and Schiavone, N. (2001) *Biochem. Biophys. Res. Commun.* **287,** 1063–1069
17. Lapucci, A., Donnini, M., Papucci, L., Witort, E., Tempestini, A., Bevilacqua, A., Nicolin, A., Brewer, G., Schiavone, N., and Capaccioli, S. (2002) *J. Biol. Chem.* **277,** 16139–16146
18. Luzi, E., Papucci, L., Schiavone, N., Donnini, M., Lapucci, A., Tempestini, A., Witort, E., Nicolin, A., and Capaccioli, S. (2003) *Cancer Gene Ther.* **10,** 201–208
19. Bevilacqua, A., Ceriani, M. C., Canti, G., Asnaghi, L., Gherzi, R., Brewer, G., Papucci, L., Schiavone, N., Capaccioli, S., and Nicolin, A. (2003) *J. Biol. Chem.* **278,** 23451–23459
20. Lee, J.-H., Takahashi, T., Yasuhara, N., Inazawa, J., Kamada, S., and Tsujimoto, Y. (1999) *Oncogene* **18,** 6183–6190
21. Thomson, A. M., Rogers, J. T., Walker, C. E., Staton, J. M., and Leedman, P. J. (1999) *BioTechniques* **27,** 1032–1042
22. Lander, E. S., Linton, L. M., Birren, B., Nusbaum, C., Zody, M. C., Baldwin, J., Devon, K., Dewar, K., Doyle, M., FitzHugh, W., Funke, R., Gage, D., Harris, K., Heaford, A., Howland, J., and *et al.* (2001) *Nature* **409,** 860–921
23. Gyapay, G., Morissette, J., Vignal, A., Dib, C., Fizames, C., Millasseau, P., Marc, S., Bernardi, G., Lathrop, M., and Weissenbach, J. (1994) *J. Nat. Genet.* **7,** 246–339
24. Dib, C., Faure, S., Fizames, C., Samson, D., Drouot, N., Vignal, A., Millasseau, P., Marc, S., Hazan, J., Seboun, E., Lathrop, M., Gyapay, G., Morissette, J., and Weissenbach, J. (1996) *Nature* **380,** 152–154
25. Pravica, V., Asderakis, A., Perrey, C., Hajeer, A., Sinnott, P. J., and Hutchinson, I. V. (1999) *Eur. J. Immunogenet.* **26,** 1–3
26. Agarwal, A. K., Giacchetti, G., Lavery, G., Nikkila, H., Palermo, M., Ricketts, M., McTernan, C., Bianchi, G., Manunta, P., Strazzullo, P., Mantero, F., White, P. C., and Stewart, P. M. (2000) *Hypertension* **36,** 187–194
27. Sharma, V. K., Rao, C. B., Sharma, A., Brahmachari, S. K., and Ramachandran, S. (2003) *Biomol. Struct. Dyn.* **21,** 303–310
28. Hui, J., Stangl, K., Lane, W. S., and Bindereif, A. (2003) *Nat. Struct. Biol.* **10,** 33–37
29. Hui, J., Reither, G., and Bindereif, A. (2003) *RNA (N. Y.)* **9,** 931–936
30. Bandyopadhyay, S., Sengupta, T. K., Fernandes, D. J., and Spicer, E. K. (2003) *Biochem. Pharmacol.* **66,** 1151–1162
31. Sengupta, T. K., Bandyopadhyay, S., Fernandes, D. J., and Spicer, E. K. (2004) *J. Biol. Chem.* **279,** 10855–10863
32. Guhaniyogi, J., and Brewer, G. (2001) *Gene (Amst.)* **265,** 11–23
33. Shih, S-C., and Claffey, K. P. (1999) *J. Biol. Chem.* **274,** 1359–1365

DECEMBER 2004 VOLUME 6 NO.12
www.nature.com/naturecellbiology

nature cell biology

Eps8 as an actin capper

Semaphorin signalling in reverse gear

A new ligase for p27^{Kip1}

nature
cell biology

Role of Bcl-2 family proteins in a non-apoptotic programmed cell death dependent on autophagy genes

Shigeomi Shimizu[1,2,3], Toku Kanaseki[4], Noboru Mizushima[4,5,6], Takeshi Mizuta[1,3], Satoko Arakawa-Kobayashi[4], Craig B. Thompson[7] and Yoshihide Tsujimoto[1,2,3,8]

Programmed cell death can be divided into several categories including type I (apoptosis) and type II (autophagic death)[1,2]. The Bcl-2 family of proteins are well-characterized regulators of apoptosis[3], and the multidomain pro-apoptotic members of this family, such as Bax and Bak, act as a mitochondrial gateway where a variety of apoptotic signals converge[4–6]. Although embryonic fibroblasts from Bax/Bak double knockout mice are resistant to apoptosis[4–6], we found that these cells still underwent a non-apoptotic death after death stimulation. Electron microscopic and biochemical studies revealed that double knockout cell death was associated with autophagosomes/autolysosomes. This non-apoptotic death of double knockout cells was suppressed by inhibitors of autophagy, including 3-methyl adenine, was dependent on autophagic proteins APG5 and Beclin 1 (capable of binding to Bcl-2/Bcl-x_L), and was also modulated by Bcl-x_L. These results indicate that the Bcl-2 family of proteins not only regulates apoptosis, but also controls non-apoptotic programmed cell death that depends on the autophagy genes.

It has been shown that cells lacking both Bax and Bak, the multidomain pro-apoptotic members of the Bcl-2 family, are completely resistant to apoptosis induced by various apoptotic stimuli, indicating that the multi-domain pro-apoptotic members act as a mitochondrial gateway for a variety of apoptotic signals[4–6]. However, although *Bax/Bak*$^{-/-}$ mice show several morphological abnormalities[4], programmed cell death seems to largely proceed in a normal manner, implying that a different mechanism compensates for apoptosis in these mice. Therefore, we investigated the response of cells from *Bax/Bak*$^{-/-}$ mice to various apoptotic stimuli in more detail.

When simian virus 40 (SV40)-transformed embryonic fibroblasts from *Bax/Bak*$^{-/-}$ mice (*Bax/Bak*$^{-/-}$ MEFs) were treated with etoposide (an inhibitor of topoisomerase II and a common apoptotic reagent), the cells became rounded, irregular and then ballooned (Fig. 1a; see Supplementary Information, Movie S1). We also continuously monitored these cells in the presence of propidium iodide (PI) (a membrane-impermeable stain for nucleic acids) under a fluorescent microscope. As shown in Fig. 1a, b and Supplementary Information, Movies S2 and S3, PI-positive cells were detected after 24 h and the majority of the cells were positively stained for PI by 48 h, indicating cell death. Note that the majority of PI-positive cells appeared to have been severely damaged. Consistently, when cell viability was assessed by the Resazurin reduction reaction using the Cell Titer Blue (CTB) assay, which measures the metabolic activity of viable cells in the same way as the MTT (methyl-thiazol-tetrazolium) assay, *Bax/Bak*$^{-/-}$ MEFs showed a significant decrease of viability (Fig. 1c). These results indicated that *Bax/Bak*$^{-/-}$ MEFs suffered a significant decrease of viability after etoposide treatment, although the extent of the change was smaller than in wild-type (WT) MEFs. As reported previously[4–6], etoposide-treated *Bax/Bak*$^{-/-}$ MEFs did not show any features of apoptosis (data not shown). Consistently, the addition of zVAD-fmk (a pan-caspase inhibitor) inhibited apoptosis of etoposide-treated WT MEFs, but did not improve the viability of *Bax/Bak*$^{-/-}$ MEFs (Fig. 1c).

To confirm the loss of cell viability after etoposide treatment, *Bax/Bak*$^{-/-}$ MEFs were exposed to etoposide, collected and re-cultured in standard medium. As shown in Fig. 1d, the proliferative activity of *Bax/Bak*$^{-/-}$ MEFs declined in a manner that was dependent on the duration of incubation with etoposide. Furthermore, the loss of cell viability was also confirmed by a clonogenicity (colony-forming) assay (Fig. 1e). Similar results were obtained when *Bax/Bak*$^{-/-}$ MEFs were treated with staurosporine (Fig. 1e and see Supplementary Information, Fig. S1a, b) or thapsigargin (data not shown). Moreover, etoposide and staurosporine induced a decrease of viability in primary *Bax/Bak*$^{-/-}$ MEFs and in thymocyte (see Supplementary Information, Fig. S1g, i, and data not shown). These results suggested that *Bax/Bak*$^{-/-}$ cells can be killed by various apoptosis-inducing reagents via a non-apoptotic process.

[1]Department of Post-Genomics & Diseases, Osaka University Medical School, [2]CREST and [3]SORST of the Japan Science and Technology Corporation (JST), 2-2 Yamadaoka, Suita, Osaka 565-0871, Japan. [4]Department of Cell Biology, National Institute for Basic Biology, and [5]PRESTO of the Japan Science and Technology Corporation (JST), Okazaki, Aichi 444-8585, Japan. [6]Department of Bioregulation and Metabolism, The Tokyo Metropolitan Institute of Medical Science, Tokyo 113-8613, Japan. [7]Departments of Medicine and Cancer Biology, Abramson Family Cancer Research Institute, University of Pennsylvania, Philadelphia, PA 19104 USA. [8]Correspondence should be addressed to: Y.T. (e-mail: tsujimot@gene.med.osaka-u.ac.jp)

Published online: 21 Novmeber 2004, DOI: 10.1038/ncb1192

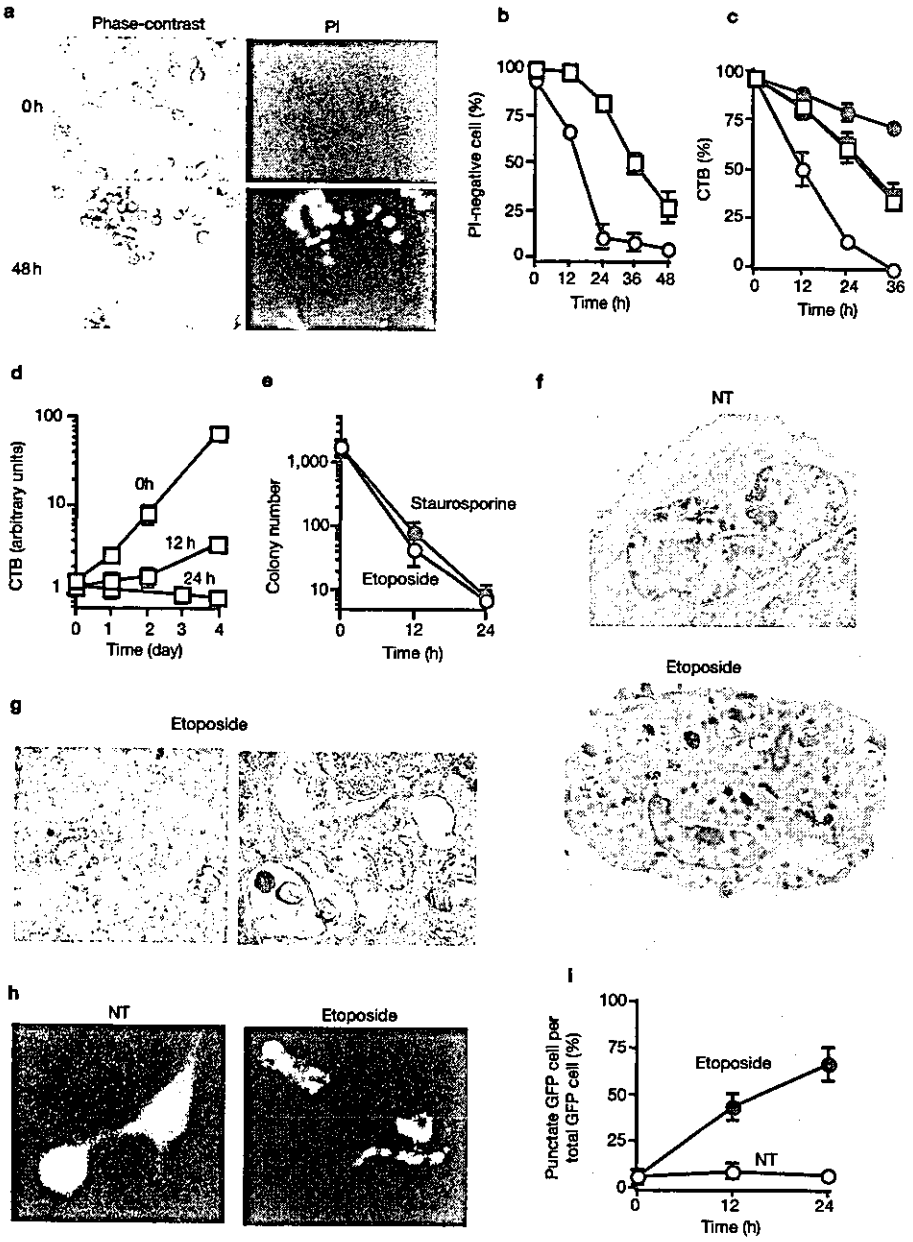

Figure 1 Loss of viability of and induction of autophagy in Bax/Bak$^{-/-}$ MEFs exposed to etoposide and staurosporine. (**a**) Representative photographs of Bax/Bak$^{-/-}$ MEFs treated with etoposide. Bax/Bak$^{-/-}$ MEFs were treated with 20 μM etoposide in the presence of PI (2 μM) for the indicated times, and were analysed under a phase-contrast and fluorescence (PI) microscope. (**b**, **c**) Reduced viability of Bax/Bak$^{-/-}$ MEFs after exposure to etoposide. WT (circles) and Bax/Bak$^{-/-}$ (squares) MEFs were treated with 20 μM etoposide in the presence (closed symbols) or absence (open symbols) of 100 μM zVAD-fmk. Then cell viability was measured by the PI staining (**b**) and CTB assay (**c**), and expressed as a percentage of the initial value without etoposide. Data are shown as mean ± s.d. ($n = 4$). (**d**) Reduced viability of etoposide-treated Bax/Bak$^{-/-}$ MEFs as assessed by proliferation assay. Bax/Bak$^{-/-}$ MEFs were either not treated (0 h) or were treated with 20 μM etoposide for 12 and 24 h, then all cells were recovered and 5,000 cells were reseeded. Viable cell numbers were measured on the indicated days by the CTB assay. Results were normalized by adjusting the day 0 value. $n = 4$. (**e**) Reduced viability of Bax/Bak$^{-/-}$ MEFs after exposure to etoposide and staurosporine, as assessed by clonogenicity assay. MEFs were treated with etoposide (20 μM) or staurosporine (1 μM) at the indicated times, collected, and 2,000 cells were seeded in the normal medium. After 1 week, colonies were counted. $n = 4$. (**f–i**) Induction of autophagy in Bax/Bak$^{-/-}$ MEFs by etoposide. (**f**) Electron micrograph (×14,800) of Bax/Bak$^{-/-}$ MEF treated with etoposide (20 μM) for 18 h. Representative features of Bax/Bak$^{-/-}$ MEFs that have received no treatment (NT; that is, are healthy) are also shown (NT: ×14,000). (**g**) In magnified photographs, a large number of autolysosomes/autophagosomes (left: ×26,000) were observed, but the mitochondria were unaffected (right: ×17,000). (**h**, **i**) Punctate GFP–LC3 fluorescence in Bax/Bak$^{-/-}$ MEFs treated with etoposide. GFP–LC3-transfected cells were incubated with and without etoposide (20 μM) for 24 h (**h**) or the indicated times (**i**), and then examined by fluorescent microscopy. (**h**) Representative photographs of healthy (NT) and etoposide-treated Bax/Bak$^{-/-}$ MEFs are shown. (**i**) The percentage of cells with punctate GFP–LC3 fluorescence was calculated relative to all GFP-positive cells. Data are shown as mean ± s.d. ($n = 4$).

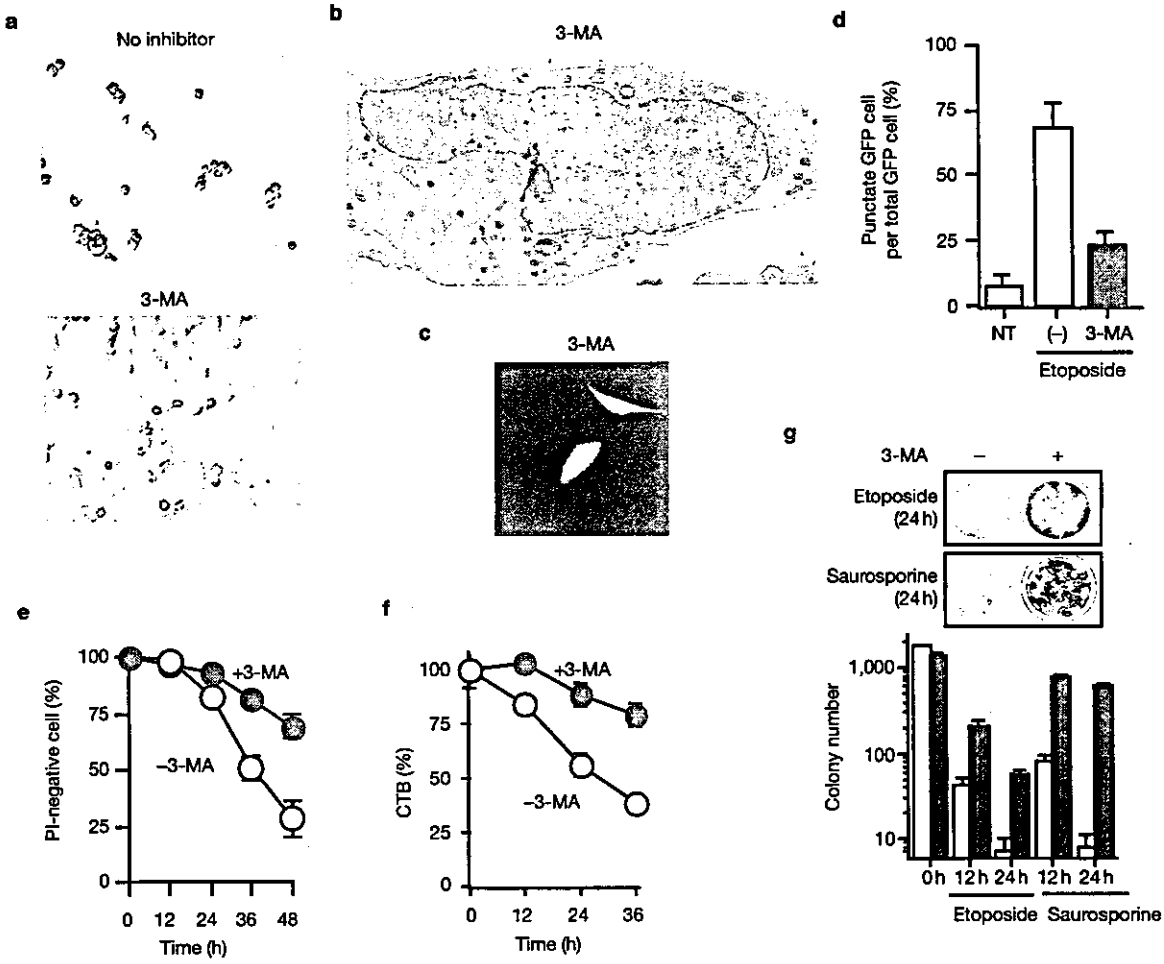

Figure 2 Inhibition of etoposide-induced death of Bax/Bak$^{-/-}$ MEFs by 3-MA. (**a**, **b**) Bax/Bak$^{-/-}$ MEFs were treated with 20 μM etoposide in the absence or presence of 10 mM 3-MA for 24 h, and then were examined by phase-contrast microscopy (**a**) and electron microscopy (×8,400) (**b**). Autolysosomes/autophagosomes were hardly observed. (**c**, **d**) Reduction of punctate GFP–LC3 fluorescence in Bax/Bak$^{-/-}$ MEFs by 3-MA. Bax/Bak$^{-/-}$ MEFs that were transfected with GFP–LC3 were incubated without (NT) or with 20 μM etoposide in the presence or absence of 10 mM 3-MA for 24 h, and then were examined by confocal fluorescent microscopy. (**c**) Representative photograph of etoposide-treated Bax/Bak$^{-/-}$ MEFs in the presence of 3-MA. (**d**) The percentage of cells with punctate GFP–LC3 fluorescence was calculated relative to all GFP–LC3-positive cells. Data are shown as mean ± s. d. ($n = 4$). (**e**–**g**) Inhibition of etoposide- and staurosporine-induced cell death by 3-MA. Bax/Bak$^{-/-}$ MEFs were treated with 20 μM etoposide (**e**–**g**) or 1 μM staurosporine (**g**) in the absence (open symbols) or presence (closed symbols) of 10 mM 3-MA for the indicated time. Cell viability was measured by PI staining (**e**), CTB assay (**f**) and clonogenicity assay (**g**) (as in Fig. 1e). Upper panels in **g**: viable cells were visualized by staining with calcein-AM. $n = 4$.

To investigate the mechanism underlying the death of *Bax/Bak*$^{-/-}$ MEFs induced by apoptotic stimuli, the cells were examined by electron microscopy. As shown in Fig. 1f, g, the majority of etoposide-treated *Bax/Bak*$^{-/-}$ MEFs, but not healthy MEFs, contained a number of autophagosomes/autolysosomes, which are a characteristic feature of autophagy. Moreover, a significant number of cells appeared to have undergone destruction by abundant autophagosomes/autolysosomes, raising the possibility that an autophagic process might be involved in the non-apoptotic death of *Bax/Bak*$^{-/-}$ MEFs. In contrast, many of the mitochondria appeared normal (Fig. 1g), although some were found inside the autophagosomes (data not shown). Although the nuclei were deformed, neither chromatin condensation nor nuclear fragmentation was observed (Fig. 1f), confirming the absence of apoptotic cell death. Autophagy is a pathway for the bulk degradation of subcellular constituents through the creation of autophagosomes/autolysosomes in response to stresses such as nutrient deprivation[7]. In general, autophagy is utilized so that cells can survive, but constitutive activation of autophagy may induce cell death. To visualize autophagy, green fluorescent protein (GFP)-tagged light-chain 3 (LC3) (ref. 8) was expressed in *Bax/Bak*$^{-/-}$ MEFs. During the autophagic process, LC3 is concentrated in autophagosomes, so the punctate fluorescence produced by GFP–LC3 can be used as a good indicator of autophagy[8]. As shown in Fig. 1h, diffuse cytoplasmic localization of GFP–LC3 was observed in healthy *Bax/Bak*$^{-/-}$ MEFs, whereas etoposide-treated *Bax/Bak*$^{-/-}$ MEFs showed punctuate fluorescence. The number of cells with punctate GFP–LC3 fluorescence increased in a time-dependent manner after etoposide treatment (Fig. 1i). Similar findings were also observed when *Bax/Bak*$^{-/-}$ MEFs were treated with staurosporine (see Supplementary Information, Fig. S1c, d). All of these results indicated that apoptotic stimuli could induce non-apoptotic death of *Bax/Bak*$^{-/-}$ MEFs, which was associated with the generation of autophagosomes/autolysosomes.

To elucidate the involvement of the autophagic process in non-apoptotic death of *Bax/Bak*$^{-/-}$ MEFs, the effects of several inhibitors of autophagy were tested. Autophagy is known to be inhibited by PI3 kinase inhibitors,

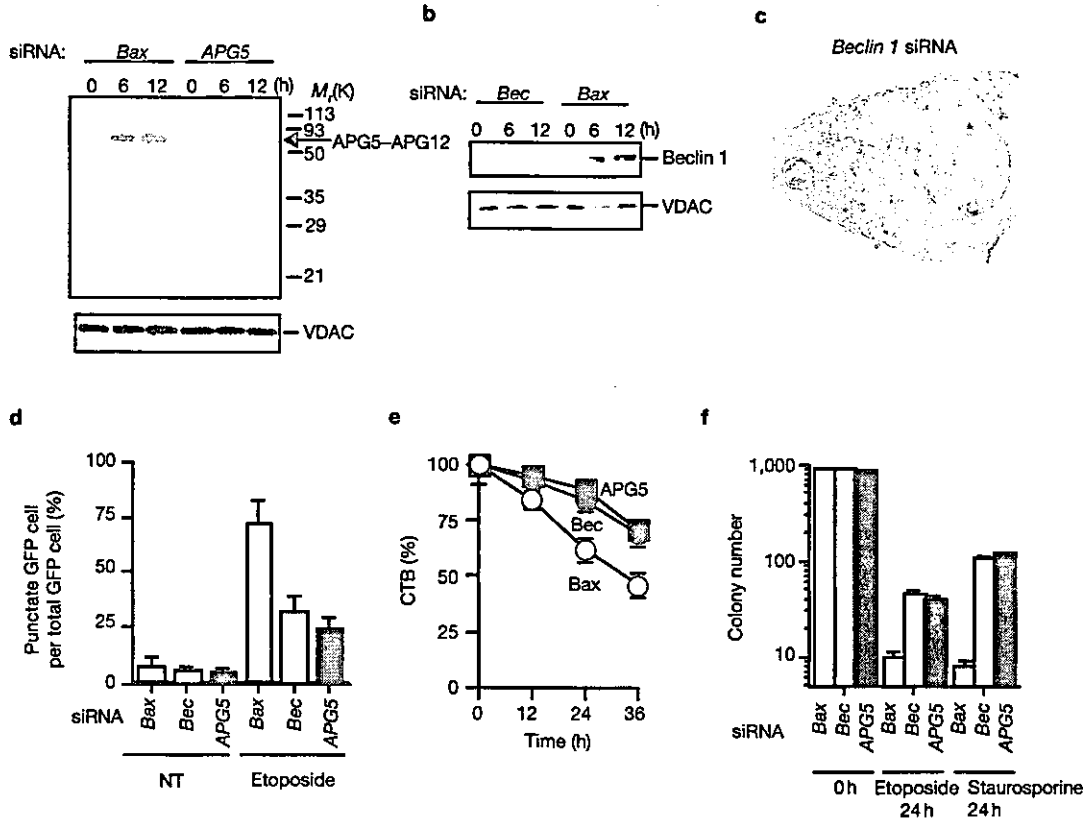

Figure 3 Inhibition of etoposide-induced death of Bax/Bak$^{-/-}$ MEFs by silencing autophagy genes. (**a**, **b**) Bax/Bak$^{-/-}$ MEFs were treated with the indicated siRNAs (10 μg) for 24 h and then incubated with 20 μM etoposide for the indicated times. Expression of APG5–APG12 complex (**a**), Beclin 1 (**b**) and VDAC (loading control) was analysed by Western blot analysis. (**c**) Inhibition of etoposide-induced autophagy by silencing of Beclin 1. Bax/Bak$^{-/-}$ MEFs with silencing of Beclin 1 were treated with 20 μM etoposide at 18 h and were analysed by electron microscopy (×8,500). (**d**) Reduction of punctate GFP–LC3 fluorescence in Bax/Bak$^{-/-}$ MEFs by silencing of Beclin 1 and APG5. Bax/Bak$^{-/-}$ MEFs that were transfected with GFP–LC3 together with the indicated siRNAs, were incubated without (NT) or with 20 μM etoposide for 24 h, and then examined by confocal fluorescent microscopy. The percentage of cells with punctate GFP–LC3 fluorescence was calculated relative to all GFP–LC3-positive cells. Data are shown as mean ± s.d. ($n = 4$). (**e**, **f**) Inhibition of etoposide- and staurosporine-induced cell death by silencing of Beclin 1 and APG5. Bax/Bak$^{-/-}$ MEFs that were treated with the indicated siRNAs were incubated with 20 μM etoposide (**e**, **f**) or 1 μM staurosporine (**f**) for the indicated time. Cell viability was measured by CTB assay (**e**) and clonogenicity assay (**f**). $n = 4$.

such as 3-methyladenine (3-MA) and wortmannin[7]. When *Bax/Bak*$^{-/-}$ MEFs were treated with etoposide in the presence of 3-MA, cell rounding and detachment were almost completely inhibited (Fig. 2a). Etoposide-induced development of autophagosomes/autolysosomes was also inhibited by 3-MA (Fig. 2b–d). Cell viability was markedly improved by 3-MA, as shown by PI staining (Fig. 2e; see Supplementary Information, Movies S4 and S5), the CTB assay (Fig. 2f) and a clonogenicity assay (Fig. 2g). Similar results were obtained with wortmannin (data not shown). Note that incubation with 3-MA or wortmannin showed only slight toxicity to cells (5–10% reduction of cell viability in 24 h). Because we used low concentrations of these drugs for all subsequent studies, toxicity should not be an issue. 3-MA also inhibited staurosporine-induced death of *Bax/Bak*$^{-/-}$ MEFs (Fig. 2g and see Supplementary Information, Fig. S1e, f), and non-apoptotic death induced by etoposide and staurosporine in primary *Bax/Bak*$^{-/-}$ MEFs and thymocytes (see Supplementary Information, Fig. S1h, i, and data not shown).

For further confirmation of the involvement of an autophagic process in the non-apoptotic death of *Bax/Bak*$^{-/-}$ MEFs, we used gene silencing with short interfering RNA (siRNA) to inhibit some genes related to the autophagic process. The protein APG5 is essential for the generation of autophagosomes by covalent binding to APG12 (ref. 9). Beclin 1 is part of a class III PI3 kinase complex that is also crucial for autophagy[10], and may function upstream of other APG proteins[11]. Interestingly, when *Bax/Bak*$^{-/-}$ MEFs were treated with etoposide, there was considerable accumulation of both the APG5–APG12 complex and Beclin 1 (Fig. 3a, b), consistent with induction of the autophagic process in etoposide-treated *Bax/Bak*$^{-/-}$ MEFs. Accumulation of Beclin 1 and the APG5–APG12 complex was inhibited by silencing of the respective genes (Fig. 3a, b). We used *Bax* siRNA as a control because Bax was absent in *Bax/Bak*$^{-/-}$ MEFs. Etoposide-induced generation of autophagosomes/autolysosomes was markedly inhibited by silencing of Beclin 1 and APG5 (Fig. 3c, d, and data not shown). Silencing of Beclin 1 and APG5 reduced the etoposide-induced death of *Bax/Bak*$^{-/-}$ MEFs (Fig. 3e, f). Similar results were obtained when cells were treated with staurosporine (Fig. 3f). All of these findings indicated that various apoptotic stimuli could induce non-apoptotic death of *Bax/Bak*$^{-/-}$ MEFs, which was dependent on autophagy genes.

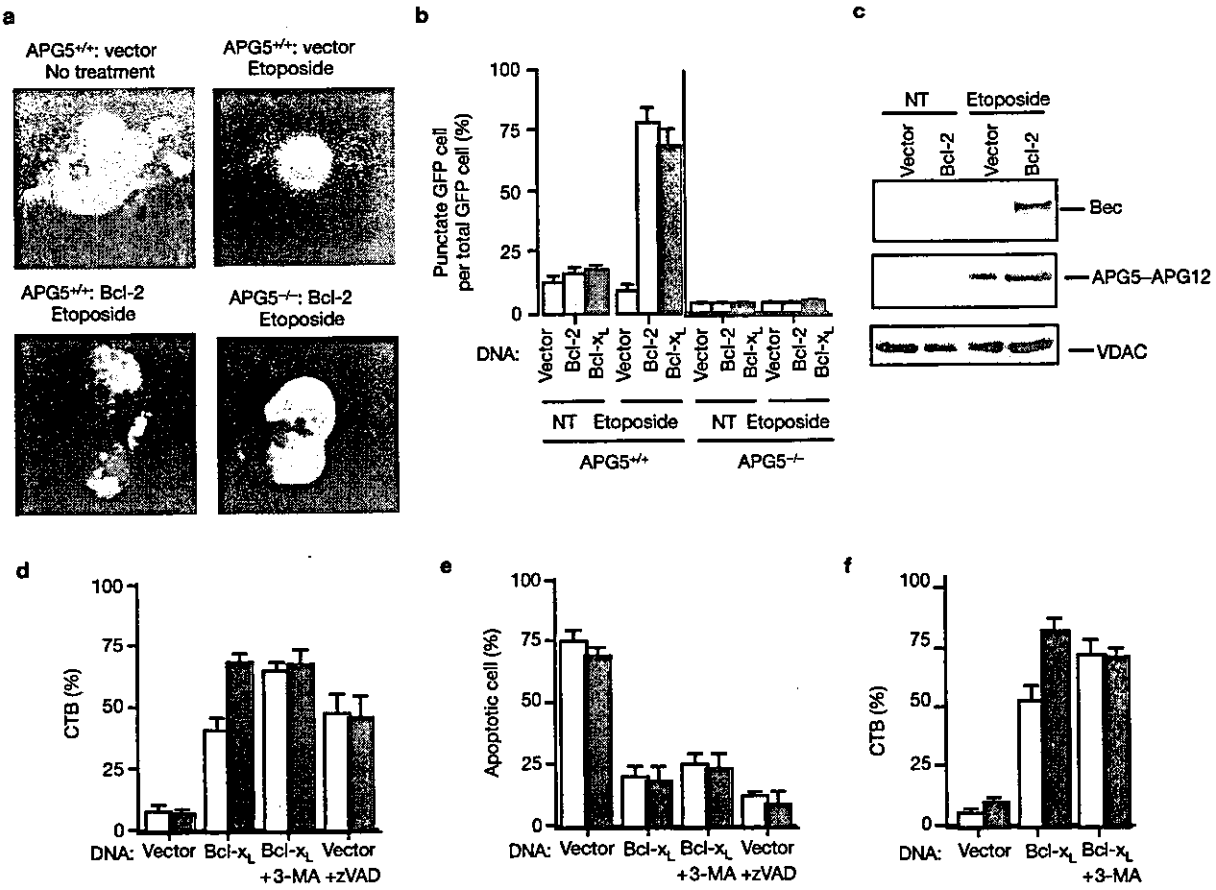

Figure 4 Occurrence of etoposide-induced, 3-MA-inhibitable, non-apoptotic death in MEFs by overexpressed Bcl-2/Bcl-x_L. (**a**, **b**) APG5-dependent punctate GFP–LC3 fluorescence in Bcl-2-transfected MEFs after etoposide treatment. $APG5^{+/+}$ and $APG5^{-/-}$ MEFs that were transfected with both GFP–LC3 and the indicated plasmids (Bcl-2 or vector) were incubated without or with 20 μM etoposide for 24 h, then examined by confocal fluorescent microscopy (**a**). The percentage of cells with punctate GFP–LC3 fluorescence was calculated relative to all GFP–LC3-positive cells (**b**). (**c**) Accumulation of Beclin 1 and APG5–APG12 complex in Bcl-2-transfected MEFs after etoposide treatment. WT MEFs were transfected with the indicated plasmids, and were incubated without (NT) or with 20 μM etoposide for 24 h. (**d**, **e**) Occurrence of etoposide-induced 3-MA-inhibitable non-apoptotic death in Bcl-x_L-overexpressing $APG5^{+/+}$ MEFs, but not $APG5^{-/-}$ MEFs. $APG5^{+/+}$ (open columns) and $APG5^{-/-}$ (closed columns) MEFs were transfected with the indicated plasmids (2 μg). After 24 h, transfected cells were incubated with 20 μM of etoposide in the presence or absence of 100 μM of zVAD or 10 mM of 3-MA for 24 h, and cell viability was measured by the CTB assay (**d**) and apoptotic nuclear morphology (**e**). Data are shown as mean ± s.d. ($n = 4$). (**f**) Overexpression of Bcl-x_L does not sensitize Beclin 1-silenced MEFs to etoposide-induced 3-MA-inhibitable non-apoptotic death. WT MEFs with silencing of control GFP (open columns) or Beclin 1 (closed columns) were transfected with the indicated plasmids (1 μg). After 24 h, transfected cells were incubated with 20 μM of etoposide in the presence or absence of 10 mM of 3-MA for 24 h, and cell viability was measured by the CTB assay. $n = 3$.

To confirm that apoptotic stimulation induced non-apoptotic cell death in *Bax/Bak*$^{-/-}$ MEFs owing to the absence of Bax and Bak, either Bax or Bak was expressed in these cells and then treatment with etoposide was performed. In contrast to *Bax/Bak*$^{-/-}$ MEFs, Bax- (or Bak)-transfected *Bax/Bak*$^{-/-}$ MEFs developed certain features of apoptosis, and were inhibited by zVAD-fmk, but not by 3-MA (see Supplementary Information, Fig. S2a, b). Thus, etoposide-induced non-apoptotic death of *Bax/Bak*$^{-/-}$ MEFs was a consequence of the inhibition of Bax/Bak activity.

To show that non-apoptotic death was not a simple consequence of the inhibition of apoptosis, we next examined non-apoptotic death in zVAD-added WT MEFs, and Apaf-1- and caspase-9-deficient MEFs after treatment with etoposide. In all cases, a small (but significant) decrease of cell viability was detected, but this decrease was not inhibited by 3-MA (see Supplementary Information, Fig. S2c–f). Furthermore, etoposide-treated WT MEFs showed only mild autophagic manifestations (see Supplementary Information, Fig. S2g–i), indicating that the 3-MA-inhibitable non-apoptotic death of *Bax/Bak*$^{-/-}$ MEFs was not merely due to inhibition of apoptosis, but was related to deficiency of both Bax and Bak.

We next examined the effect of overexpression of Bcl-2 and Bcl-x_L in WT MEFs. These cells were expected to undergo 3-MA-inhibitable non-apoptotic death, as do *Bax/Bak*$^{-/-}$ MEFs in response to apoptotic stimulations. MEFs overexpressing Bcl-2 (and also Bcl-x_L) showed punctuate GFP–LC3 fluorescence (Fig. 4a, b) and greater accumulation of Beclin 1 and APG5–APG12 complex after etoposide treatment than did WT MEFs (Fig. 4c). This punctuate GFP–LC3 fluorescence was not observed in *APG5*$^{-/-}$ MEFs (Fig. 4a, b), in which autophagy was impaired[18], indicating that overexpression of Bcl-2/Bcl-x_L induced APG5-dependent autophagy in WT MEFs after etoposide treatment. To confirm that cells overexpressing Bcl-2/Bcl-x_L undergo etoposide-induced non-apoptotic death, *APG5*$^{-/-}$ MEFs were transfected with a